Inorganic Chemistry
Article

Inorg. Chem. **2009**, *48*, 6011–6025 **6011**
DOI: 10.1021/ic900412n

Synthesis, Properties, and Live-Cell Imaging Studies of Luminescent Cyclometalated Iridium(III) Polypyridine Complexes Containing Two or Three Biotin Pendants

Kenneth Yin Zhang and Kenneth Kam-Wing Lo*

Department of Biology and Chemistry, City University of Hong Kong, Tat Chee Avenue, Kowloon, Hong Kong, People's Republic of China

Received February 28, 2009

Three luminescent cyclometalated iridium(III) bis-biotin complexes $[Ir(N^{\wedge}C)_2(N^{\wedge}N)](PF_6)$ (HN^C = 2-(4-(*N*-(6-(biotinamido)hexyl)aminomethyl)phenyl)pyridine, HppyC6B, N^N = 2,2′-bipyridine, bpy (**1**); HN^C = 2-phenylpyridine, Hppy, N^N = 4,4′-bis((2-(biotinamido)ethyl)aminocarbonyl)-2,2′-bipyridine, bpyC2B2 (**2**); HN^C = Hppy, N^N = 4,4′-bis((2-((6-(biotinamido)hexanoyl)amino)ethyl)aminocarbonyl)-2,2′-bipyridine, bpyC2C6B2 (**3**)) and one tris-biotin complex $[Ir(ppyC6B)_2(bpyC6B)](PF_6)$ (bpyC6B = 4-((6-(biotinamido)hexyl)aminocarbonyl)-4′-methyl-2,2′-bipyridine) (**4**) have been synthesized and characterized. The biotin-free complex $[Ir(ppy)_2(bpyC4)](PF_6)$ (bpyC4 = 4,4′-bis(*n*-butylaminocarbonyl)-2,2′-bipyridine) (**5**) has also been prepared for comparison studies. Upon photoexcitation, all the complexes displayed intense and long-lived greenish-yellow to red triplet metal-to-ligand charge-transfer (^{3}MLCT) ($d\pi$ (Ir) $\rightarrow \pi^*$(N^N)) emission in fluid solutions at room temperature and in low-temperature glass. Cyclic voltammetric studies revealed iridium(IV/III) oxidation at about +1.21 to + 1.29 V and diimine-based reductions at about −1.07 to −1.39 V versus SCE. The interactions of the bis-biotin and tris-biotin complexes with avidin have been studied by 4′-hydroxyazobenzene-2-carboxylic acid (HABA) assays, emission titrations, and dissociation assays. The possibility of these complexes as cross-linkers for avidin has been examined by microscopy studies using avidin-conjugated green fluororescent microspheres and size-exclusion HPLC analysis. Utilization of these luminescent iridium(III) biotin complexes in signal amplification has been demonstrated using avidin-coated nonfluorescent microspheres and complex **3** as an example. Additionally, the lipophilicity of all the complexes has been determined by reversed-phase HPLC. The cytotoxicity of these iridium(III) complexes toward the human cervix epithelioid carcinoma (HeLa) cell line has been evaluated by 3-(4,5-dimethyl-2-thiazolyl)-2,5-diphenyltetrazolium bromide (MTT) assays. Furthermore, the cellular uptake of the complexes has been examined by ICP-MS, laser-scanning confocal microscopy, and flow cytometry.

Introduction

The avidin−biotin system is widely utilized in immunology, histochemistry, and in situ hybridization.[1−4] The biological properties of common biomolecules are usually retained after modification with biotin (biotinylation). Also, the four biotin-binding sites of avidin allow the use of multibiotin reagents to cross-link reporter-labeled avidin, resulting in signal amplification. For example, ^{125}I-labeled recombinant streptavidin (rSAv) has been cross-linked with organic multibiotin compounds to yield streptavidin−biotin complexes, which offer much higher radioactivity than a single ^{125}I-rSAv molecule.[5a,5b] Similar signal amplification has also been achieved using streptavidin, biotin, and lanthanide chelates in a macromolecular approach.[5c] In view of the interesting

*To whom correspondence should be addressed. E-mail: bhkenlo@cityu.edu.hk. Phone: (852) 2788 7231. Fax: (852) 2788 7406.

(1) Hermanson, G. T. *Bioconjugate Techniques*; Academic Press: San Diego, CA, 1996.
(2) Wilchek, M.; Bayer, E. A. *Methods in Enzymology*; Academic Press: San Diego, CA, 1990; Vol. 184.
(3) Wilchek, M.; Bayer, E. A. *Anal. Biochem.* **1988**, *171*, 1–32.
(4) (a) Green, N. M. *Adv. Protein Chem.* **1975**, *29*, 85–133. (b) Green, N. M. *Methods Enzymol.* **1990**, *184*, 51–67.
(5) (a) Wilbur, D. S.; Pathare, P. M.; Hamlin, D. K.; Weerawarna, S. A. *Bioconjugate Chem.* **1997**, *8*, 819–832. (b) Wilbur, D. S.; Pathare, P. M.; Hamlin, D. K.; Buhler, K. R.; Vessella, R. L. *Bioconjugate Chem.* **1998**, *9*, 813–825. (c) Morton, R. C.; Diamandis, E. P. *Anal. Chem.* **1990**, *62*, 1841–1845.
(6) (a) Sprouse, S.; King, K. A.; Spellane, P. J.; Watts, R. J. *J. Am. Chem. Soc.* **1984**, *106*, 6647–6653. (b) King, K. A.; Spellane, P. J.; Watts, R. J. *J. Am. Chem. Soc.* **1985**, *107*, 1431–1432. (c) King, K. A.; Watts, R. J. *J. Am. Chem. Soc.* **1987**, *109*, 1589–1590.
(7) (a) Didier, P.; Ortmans, I.; Kirsch-De Mesmaeker, A.; Watts, R. J. *Inorg. Chem.* **1993**, *32*, 5239–5245. (b) Ortmans, I.; Didier, P.; Kirsch-De Mesmaeker, A. *Inorg. Chem.* **1995**, *34*, 3695–3704.
(8) (a) Holder, E.; Marin, V.; Kozodaev, D.; Meier, M. A. R.; Lohmeijer, B. G. G.; Schubert, U. S. *Macromol. Chem. Phys.* **2005**, *206*, 989–997. (b) Holfer, E.; Marin, V.; Alexeev, A.; Schubert, U. S. *J. Polym. Sci. Pol. Chem.* **2005**, *43*, 2765–2776. (c) Marin, V.; Holder, E.; Hoogenboom, R.; Tekin, E.; Schubert, U. S. *Dalton Trans.* **2006**, 1636–1644.

Published on Web 05/29/2009

emissive behavior of iridium(III) polypyridine complexes, in particular their high environment-sensitivity and diverse emissive-state character,[6−24] we have designed luminescent cyclometalated iridium(III) complexes as biological covalent labels[24a−24e,24g,24o] and noncovalent probes,[24f,24h−24j,24l−24s] including a series of biotin-containing complexes.[24f,24h−24j,24l,24m,24o−24q]

We herein report the synthesis and various properties of three new iridium(III) bis-biotin complexes $[Ir(N^{\wedge}C)_2(N^{\wedge}N)](PF_6)$ (HN^C = 2-(4-(*N*-(6-(biotinamido)hexyl)aminomethyl)phenyl)pyridine, HppyC6B, N^N = 2,2′-bipyridine, bpy (**1**); HN^C = 2-phenylpyridine, Hppy, N^N = 4,4′-bis-((2-(biotinamido)ethyl)aminocarbonyl)-2,2′-bipyridine, bpyC2B2 (**2**); HN^C = Hppy, N^N = 4,4′-bis((2-((6-(biotinamido) hexanoyl)amino)ethyl)aminocarbonyl)-2,2′-bipyridine, bpyC2C6B2 (**3**)), one tris-biotin complex $[Ir(ppyC6B)_2(bpyC6B)](PF_6)$ (bpyC6B = 4-((6-(biotinamido)hexyl)aminocarbonyl)-4′-methyl-2,2′-bipyridine) (**4**), and one biotin-free complex $[Ir(ppy)_2(bpyC4)](PF_6)$ (bpyC4 = 4,4′-bis(*n*-butylaminocarbonyl)-2,2′-bipyridine) (**5**) (Chart 1). Additionally, the interactions of the biotin complexes **1**−**4** with avidin have been studied by spectroscopy, microscopy, and chromatography methods. We have previously studied the avidin-binding properties of four iridium(III) bis-biotin complexes.[24l] In the current work, we have set our targets on the following studies: (1) the effects of spacer-arms and locations of biotin units on the photophysical, lipophilic, and avidin-binding properties of the new bis- and tris-biotin complexes, (2) the possibility of these complexes as cross-linkers for avidin, and their use in signal amplification for hetergeneous

(9) (a) Collin, J.-P.; Dixon, I. M.; Sauvage, J.-P.; Williams, J. A. G.; Barigelletti, F.; Flamigni, L. *J. Am. Chem. Soc.* **1999**, *121*, 5009–5016. (b) Dixon, I. M.; Collin, J.-P.; Sauvage, J.-P.; Flamigni, L.; Encinas, S.; Barigelletti, F. *Chem. Soc. Rev.* **2000**, *29*, 385–391. (c) Auffrant, A.; Barbieri, A.; Barigelletti, F.; Lacour, J.; Mobian, P.; Collin, J.-P.; Sauvage, J.-P.; Ventura, B. *Inorg. Chem.* **2007**, *46*, 6911–6919.

(10) (a) Griffiths, P. M.; Loiseau, F.; Puntoriero, F.; Serroni, S.; Campagna, S. *Chem. Commun.* **2000**, 2297–2298. (b) Neve, F.; Crispini, A.; Serroni, S.; Loiseau, F.; Campagna, S. *Inorg. Chem.* **2001**, *40*, 1093–1101. (c) Neve, F.; La Deda, M.; Crispini, A.; Bellusci, A.; Puntoriero, F.; Campagna, S. *Organometallics* **2004**, *23*, 5856–5863. (d) Neve, F.; La Deda, M.; Puntoriero, F.; Campagna, S. *Inorg. Chim. Acta* **2006**, *359*, 1666–1672. (e) Natstasi, F.; Puntoriero, F.; Campagna, S.; Schergna, S.; Maggini, M.; Cardinali, F.; Delavaux-Nicot, B.; Nierengarten, J.-F. *Chem. Commun.* **2007**, 3556–3558.

(11) (a) Tamayo, A. B.; Alleyne, B. D.; Djurovich, P. I.; Lamansky, S.; Tsyba, I.; Ho, N. N.; Bau, R.; Thompson, M. E. *J. Am. Chem. Soc.* **2003**, *125*, 7377–7387. (b) Wang, X.; Li, J.; Thompson, M. E.; Zink, J. I. *J. Phys. Chem. A* **2007**, *111*, 3256–3262. (c) Hirani, B.; Li, J.; Djurovich, P. I.; Yousufuddin, M.; Oxgaard, J.; Persson, P.; Wilson, S. R.; Bau, R.; Goddard, W. A.III; Thompson, M. E. *Inorg. Chem.* **2007**, *46*, 3865–3875. (d) Finkenzeller, W. J.; Hofbeck, T.; Thompson, M. E.; Yersin, H. *Inorg. Chem.* **2007**, *46*, 5076–5083.

(12) (a) De Angelis, F.; Fantacci, S.; Evans, N.; Klein, C.; Zakeeruddin, S. M.; Moser, J.-E.; Kalyanasundaram, K.; Bolink, H. J.; Grätzel, M.; Nazeeruddin, M. K. *Inorg. Chem.* **2007**, *46*, 5989–6001. (b) Di Censo, D.; Fantacci, S.; De Angelis, F.; Klein, C.; Evans, N.; Kalyanasundaram, K.; Bolink, H. J.; Grätzel, M.; Nazeeruddin, M. K. *Inorg. Chem.* **2008**, *47*, 980–989. (c) Baranoff, E.; Suàrez, S.; Bugnon, P.; Barolo, C.; Buscaino, R.; Scopelliti, R.; Zuppiroli, L.; Graetzel, M.; Nazeeruddin, Md. K. *Inorg. Chem.* **2008**, *47*, 6575–6577.

(13) (a) Wilkinson, A. J.; Goeta, A. E.; Foster, C. E.; Williams, J. A. G. *Inorg. Chem.* **2004**, *43*, 6513–6515. (b) Wilkinson, A. J.; Puschmann, H.; Howard, J. A. K.; Foster, C. E.; Williams, J. A. G. *Inorg. Chem.* **2006**, *45*, 8685–8699. (c) Williams, J. A. G.; Wilkinson, A. J.; Whittle, V. L. *Dalton Trans.* **2008**, 2081–2099. (d) Whittle, V. L.; Williams, J. A. G. *Inorg. Chem.* **2008**, *47*, 6596–6607.

(14) (a) Polson, M.; Fracasso, S.; Bertolasi, V.; Ravaglia, M.; Scandola, F. *Inorg. Chem.* **2004**, *43*, 1950–1956. (b) Polson, M.; Ravaglia, M.; Fracasso, S.; Garavelli, M.; Scandola, F. *Inorg. Chem.* **2005**, *44*, 1282–1289.

(15) (a) Coppo, P.; Duati, M.; Kozhevnikov, V. N.; Hofstraat, J. W.; De Cola, L. *Angew. Chem., Int. Ed.* **2005**, *44*, 1806–1810. (b) Avilov, I.; Minoofar, P.; Cornil, J.; De Cola, L. *J. Am. Chem. Soc.* **2007**, *129*, 8247–8258. (c) Orselli, E.; Kottas, G. S.; Konradsson, A. E.; Coppo, P.; Frohlich, R.; Frtshlich, R.; De Cola, L.; van Dijken, A.; Buchel, M.; Borner, H. *Inorg. Chem.* **2007**, *46*, 11082–11093. (d) Orselli, E.; Albuquerque, R. Q.; Fransen, P. M.; Fröhlich, R.; Janssenc, H. M.; De Cola, L. *J. Mater. Chem.* **2008**, *18*, 4579–4590. (e) Mehlstäubl, M.; Kottas, G. S.; Colella, S.; De Cola, L. *Dalton Trans.* **2008**, 2385–2388. (f) Guerrero-Martínez, A.; Vida, Y.; Domínguez-Gutiérrez, D.; Albuquerque, R. Q.; De Cola, L. *Inorg. Chem.* **2008**, *47*, 9131–9133. (g) Stagni, S.; Colella, S.; Palazzi, A.; Valenti, G.; Zacchini, S.; Paolucci, F.; Marcaccio, M.; Albuquerque, R. Q.; De Cola, L. *Inorg. Chem.* **2008**, *47*, 10509–10521.

(16) (a) Yutaka, T.; Obara, S.; Ogawa, S.; Nozaki, K.; Ikeda, N.; Ohno, T.; Ishii, Y.; Sakai, K.; Haga, M. *Inorg. Chem.* **2005**, *44*, 4737–4746. (b) Obara, S.; Itabashi, M.; Okuda, F.; Tamaki, S.; Tanabe, Y.; Ishii, Y.; Nozaki, K.; Haga, M. *Inorg. Chem.* **2006**, *45*, 8907–8921. (c) Yang, L.; Okuda, F.; Kobayashi, K.; Nozaki, K.; Tanabe, Y.; Ishii, Y.; Haga, M. *Inorg. Chem.* **2008**, *47*, 7154–7165.

(17) (a) Lowry, M. S.; Bernhard, S. *Chem.—Eur. J.* **2006**, *12*, 7970–7977. (b) Zysman-Colman, E.; Slinker, J. D.; Parker, J. B.; Malliaras, G. G.; Bernhard, S. *Chem. Mater.* **2008**, *20*, 388–396. (c) Coughlin, F. J.; Westrol, M. S.; Oyler, K. D.; Byrne, N.; Kraml, C.; Zysman-Colman, E.; Lowry, M. S.; Bernhard, S. *Inorg. Chem.* **2008**, *47*, 2039–2048.

(18) (a) Chou, P.-T.; Chi, Y. *Chem.—Eur. J.* **2007**, *13*, 380–395. (b) Fang, C.-H.; Chen, Y.-L.; Yang, C.-H.; Chi, Y.; Yeh, Y.-S.; Li, E. Y.; Cheng, Y.-M.; Hsu, C.-J.; Chou, P.-T.; Chen, C.-T. *Chem.—Eur. J.* **2007**, *13*, 2686–2694. (c) Yang, C.-H.; Cheng, Y.-M.; Chi, Y.; Hsu, C.-J.; Fang, F.-C.; Wong, K.-T.; Chou, P.-T.; Chang, C.-H.; Tsai, M.-H.; Wu, C. C. *Angew. Chem., Int. Ed.* **2007**, *46*, 2418–2421. (d) Chang, C.-F.; Cheng, Y.-M.; Chi, Y.; Chiu, Y.-C.; Lin, C.-C.; Lee, G.-H.; Chou, P.-T.; Chen, C.-C.; Chang, C.-H.; Wu, C. C. *Angew. Chem., Int. Ed.* **2008**, *47*, 4542–4545.

(19) (a) Liu, S.-J.; Zhao, Q.; Chen, R.-F.; Deng, Y.; Fan, Q.-L.; Li, F.-Y.; Wang, L.-H.; Huang, C.-H.; Huang, W. *Chem.—Eur. J.* **2006**, *12*, 4351–4361. (b) Li, X.; Chen, Z.; Zhao, Q.; Shen, L.; Li, F.; Yi, T.; Cao, Y.; Huang, C. *Inorg. Chem.* **2007**, *46*, 5518–5527. (c) Liu, Z.; Nie, D.; Bian, Z.; Chen, F.; Lou, B.; Bian, J.; Huang, C. *ChemPhysChem* **2008**, *9*, 634–640. (d) Zhao, Q.; Li, L.; Li, F.; Yu, M.; Liu, Z.; Yi, T.; Huang, C. *Chem. Commun.* **2008**, 685–687. (e) Yu, M.; Zhao, Q.; Shi, L.; Li, F.; Zhou, Z.; Yang, H.; Yi, T.; Huang, C. *Chem. Commun.* **2008**, 2115–2117.

(20) Dragonetti, C.; Falciola, L.; Mussini, P.; Righetto, S.; Roberto, D.; Ugo, R.; Valore, A.; De Angelis, F.; Fantacci, S.; Sgamellotti, A.; Ramon, M.; Muccini, M. *Inorg. Chem.* **2007**, *46*, 8533–8547.

(21) Zeng, X.; Tavasli, M.; Perepichka, I. F.; Batsanov, A. S.; Bryce, M. R.; Chiang, C.-J.; Rothe, C.; Monkman, A. P. *Chem.—Eur. J.* **2008**, *14*, 933–943.

(22) Freys, J. C.; Bernardinellib, G.; Wenger, O. S. *Chem. Commun.* **2008**, 4267–4269.

(23) Kwon, T.-H.; Kwon, J.; Hong, J.-I. *J. Am. Chem. Soc.* **2008**, *130*, 3726–3727.

(24) (a) Lo, K. K.-W.; Ng, D. C.-M.; Chung, C.-K. *Organometallics* **2001**, *20*, 4999–5001. (b) Lo, K. K.-W.; Chung, C.-K.; Ng, D. C.-M.; Zhu, N. *New J. Chem.* **2002**, *26*, 81–88. (c) Lo, K. K.-W.; Chung, C.-K.; Zhu, N. *Chem.—Eur. J.* **2003**, *9*, 475–483. (d) Lo, K. K.-W.; Chung, C.-K.; Lee, T. K.-M.; Lui, L.-H.; Tsang, K. H.-K.; Zhu, N. *Inorg. Chem.* **2003**, *42*, 6886–6897. (e) Lo, K. K.-W.; Chan, J. S.-W.; Chung, C.-K.; Tsang, V. W.-H.; Zhu, N. *Inorg. Chim. Acta* **2004**, *357*, 3109–3118. (f) Lo, K. K.-W.; Chan, J. S.-W.; Lui, L.-H.; Chung, C.-K. *Organometallics* **2004**, *23*, 3108–3116. (g) Lo, K. K.-W.; Hui, W.-K.; Chung, C.-K.; Tsang, K. H.-K.; Ng, D. C.-M.; Zhu, N.; Cheung, K.-K. *Coord. Chem. Rev.* **2005**, *249*, 1434–1450. (h) Lo, K. K.-W.; Li, C.-K.; Lau, J. S.-Y. *Organometallics* **2005**, *24*, 4594–4601. (i) Lo, K. K.-W.; Chung, C- K.; Zhu, N. *Chem.—Eur. J.* **2006**, *12*, 1500–1512. (j) Lo, K. K.-W.; Hui, W.-K.; Chung, C.-K.; Tsang, K. H.-K.; Lee, T. K.-M.; Li, C.-K.; Lau, J. S.-Y.; Ng, D. C.-M. *Coord. Chem. Rev.* **2006**, *250*, 1724–1736. (k) Lo, K. K.-W.; Lau, J. S.-Y.; Lo, D. K.-K.; Lo, L. T.-L. *Eur. J. Inorg. Chem.* **2006**, 4054–4062. (l) Lo, K. K.-W.; Lau, J. S.-Y. *Inorg. Chem.* **2007**, *46*, 700–709. (m) Lo, K. K.-W.; Tsang, K. H.-K.; Sze, K.-S.; Chung, C.-K.; Lee, T. K.-M.; Zhang, K. Y.; Hui, W.-K.; Li, C.-K.; Lau, J. S.-Y.; Ng, D. C.-M.; Zhu, N. *Coord. Chem. Rev.* **2007**, *251*, 2292–2310. (n) Lo, K. K.-W; Zhang, K. Y.; Chung, C.-K.; Kwok, K. Y. *Chem.—Eur. J.* **2007**, *13*, 7110–7130. (o) Lo, K. K.-W. *Struct. Bonding (Berlin)* **2007**, *123*, 205–245. (p) Lo, K. K.-W.; Lau, J. S.-Y. *Coordination Chemistry Research Trends*; Nova Publishers: New York, 2008; pp 175−220.(q) Lo, K. K.-W.; Zhang, K. Y.; Leung, S.-K.; Tang, M.-C. *Angew. Chem., Int. Ed.* **2008**, *47*, 2213–2216. (r) Lo, K. K.-W.; Lee, P.-K.; Lau, J. S.-Y. *Organometallics* **2008**, *27*, 2998–3006. (s) Lau, J. S.-Y.; Lee, P.-K.; Tsang, K. H.-K.; Ng, C. H.-C.; Lam, Y.-W.; Cheng, S.-H.; Lo, K. K.-W. *Inorg. Chem.* **2009**, *48*, 708–718.

Chart 1. Structures of Complexes **1**−**5**

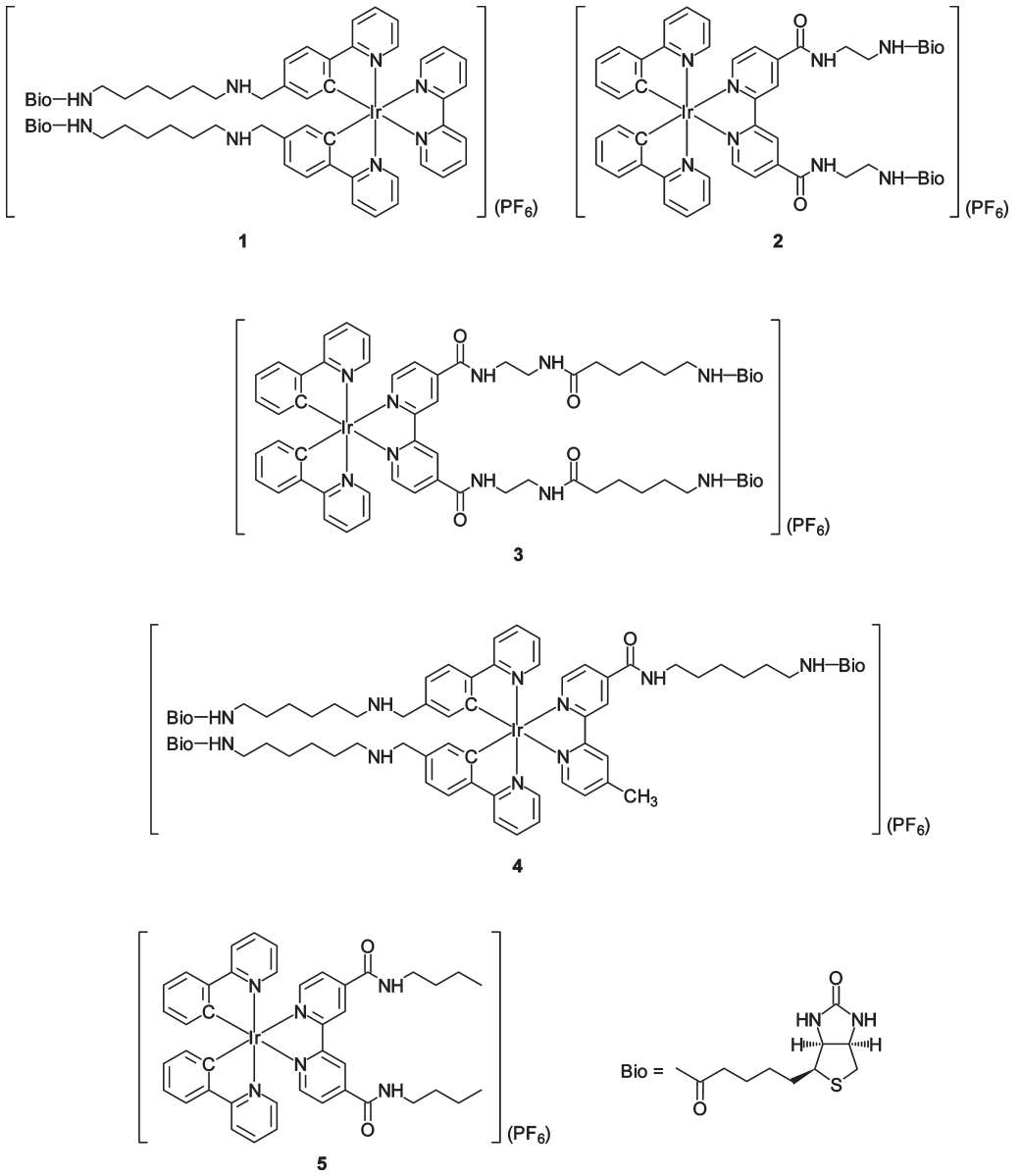

bioassays, and (3) the cytotoxicity and cellular uptake properties of the complexes, with an emphasis on live-cell imaging applications. The use of luminescent transition metal complexes for live-cell imaging is an exciting area of research because of the interesting emission properties and wide structural variety of these complexes, which may be useful in the development of organelle-specific luminescent probes. Also, it is conceivable that the rich photochemical properties (in particular, the photoredox behavior) of many luminescent transition metal complexes can be exploited in the design of intracellular reagents for photodynamic therapy.

Results and Discussion

Complex Design and Synthesis. We are interested in using bis(cyclometalated) iridium(III) diimine complexes of the general formula $[Ir(N^{\wedge}C)_2(N^{\wedge}N)]^+$ in the design of biological probes.[24a,24c−24j,24l−24s] Since one of the targets of the current work is to design new luminescent multiple-biotin reagents as cross-linkers for avidin, we used C2 and C6 spacer-arms to separate the biotin units to reduce steric hindrance between protein molecules.[24l,24n,24s] Also, an interesting study has shown that to maximize the degree of protein cross-linking, reagents containing three biotins are particularly effective.[5a] The reason is that even if two of the biotins bind to the same avidin, the third biotin can preferentially bind to another protein molecule if the length of the spacer-arms is appropriate. In general, the complexes $[Ir(N^{\wedge}C)_2(N^{\wedge}N)]^+$ are commonly synthesized by refluxing the dimer $[Ir_2(N^{\wedge}C)_4Cl_2]$ with $N^{\wedge}N$ in a mixture of CH_2Cl_2 and MeOH. Herein, the biotin units were introduced to complexes **1**−**4** by two methods: (1) the aldehyde groups of $[Ir(pba)_2(N^{\wedge}N)](PF_6)$ (pba = 4-(2-pyridyl)benzaldehyde) were conjugated with two biotin units by reaction with *N*-biotinyl-1,6-diaminohexane in the presence of $NaBH_4$; (2) 4,4′-dimethyl-2,2′-bipyridine was oxidized to 4-carboxyl-4′-methyl-2,2′-bipyridine and 4,4′-dicarboxyl-2,2′-bipyridine by SeO_2/Ag_2O and CrO_3, respectively, which were modified with one and two amine-containing biotin compounds to yield

Table 1. Electronic Absorption Spectral Data of Complexes **1**−**5** at 298 K

complex	medium	λ_{abs}/nm (ε/dm^3 mol^{-1} cm^{-1})
1	CH_2Cl_2	259 sh (41,425), 271 (41,895), 309 sh (22,770), 383 sh (6,380), 408 sh (4,355), 470 sh (780)
	CH_3CN	257 (43,575), 267 sh (43,405), 308 sh (23,275), 373 sh (5,800), 406 sh (3,930), 469 sh (640)
	MeOH	257 (49,700), 269 sh (48,645), 310 sh (24,810), 375 sh (6,175), 406 sh (4,190), 468 sh (690)
2	CH_3CN	254 (35,350), 271 sh (31,005), 291 sh (23,375), 325 sh (12,890), 366 (6,915), 486 (835)
	MeOH	254 (40,595), 271 sh (35,925), 296 sh (25,660), 327 sh (13,660), 372 (8,035), 487 (825)
3	CH_3CN	254 (32,240), 271 sh (28,635), 292 sh (21,450), 329 sh (10,255), 368 (6,280), 487 (725)
	MeOH	253 (41,605), 269 sh (37,490), 292 sh (28,410), 324 sh (14,940), 371 (7,700), 486 (790)
4	MeOH	256 (47,350), 271 sh (45,385), 314 sh (22,770), 379 sh (7,310), 409 sh (4,230), 471 sh (960)
5	CH_2Cl_2	256 (39,900), 273 sh (35,305), 296 sh (26,820), 325 sh (13,940), 376 (7,525), 487 sh (715)
	CH_3CN	254 (37,905), 272 sh (32,380), 293 sh (23,780), 323 sh (13,380), 363 (7,275), 384 sh (6,300), 489 sh (675)
	MeOH	253 (35,940), 269 sh (31,950), 294 sh (23,445), 324 sh (12,720), 372 (6,840), 487 sh (650)

the diimine ligands bpyC6B, bpyC2B2, and bpyC2-C6B2. Complexes **1**−**5** were purified by recrystallization, characterized by ^{1}H NMR spectroscopy, positive-ion ESI-MS, and IR spectroscopy, and gave satisfactory microanalysis. The color of the complexes depends on the number of amide groups on the bipyridine ligand. Complex **1**, with an unmodified bpy ligand, is yellow in color; complex **4**, whose bpy is functionalized with one electron-withdrawing amide group, is orange in color; complexes **2**, **3**, and **5**, which possess two amide groups directly appended to bpy, are orange-red to red in color.

Electronic Absorption Spectroscopy. The electronic absorption spectral data of all the complexes are listed in Table 1. The electronic absorption spectra of complexes **1** and **2** in CH_3CN at 298 K are shown in Figure 1. All the complexes showed intense spin-allowed intraligand (^{1}IL) ($\pi \rightarrow \pi^*$) (N^N and N^C) absorption bands and shoulders at about 253−329 nm (ε on the order of 10^4 dm^3 mol^{-1} cm^{-1}) and less intense spin-allowed metal-to-ligand charge-transfer (^{1}MLCT) (dπ (Ir) $\rightarrow \pi^*$(N^N and N^C)) transition bands and shoulders at >350 nm, respectively.[6a,7−10,11a,11c,11d,12−14,15a,15c−15g,16−18,19a−19d,20,21,23,24a−24n,24r,24s] However, the mixing of ligand-to-ligand charge-transfer (^{1}LLCT)[10c,10d,14,24n] (N^C $\rightarrow$ N^N) and sigma-bond-to-ligand charge-transfer (^{1}SBLCT)[7,10c,24a,24d,24n] (σ(Ir−C) $\rightarrow \pi^*$(N^N)) character in the latter transitions cannot be excluded. Additionally, all the complexes displayed weak absorption tailing at about 450−550 nm, which have been assigned to spin-forbidden ^{3}CT (dπ (Ir) $\rightarrow \pi^*$ (N^N and N^C)) transitions.[8a,8b,9a,9c,10,11a,11d,13a,13b,13d,-15c−15e,15g,17a,17c,18b,19a−19d,21,24a−24n,24r,24s] Complexes **2**, **3**, and **5**, of which the π^* orbitals of the bpy ligands are stabilized by two electron-withdrawing amide groups, displayed a lower-energy ^{1}CT band or shoulder (ca. 486−489 nm) compared to those of complexes **1** and **4** (ca. 468−471 nm) (Table 1).

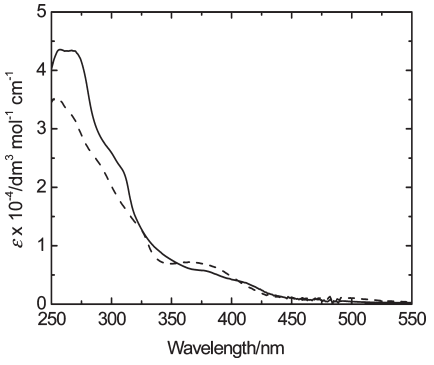

Figure 1. Electronic absorption spectra of complexes **1** (solid line) and **2** (dashed line) in CH_3CN at 298 K.

Table 2. Photophysical Data of Complexes **1**−**5**[a]

complex	medium (T/K)	λ_{em}/nm	τ_o/μs	Φ_{em}
1	CH_2Cl_2 (298)	578	0.45	0.22
	CH_3CN (298)	587	0.25	0.050
	MeOH (298)	585	0.26	0.16
	buffer[b] (298)	569	0.22	0.19
	glass[c] (77)	512, 539 sh	5.24	
2	CH_3CN (298)	633	0.10	0.017
	MeOH (298)	650	0.041	0.0064
	buffer[b] (298)	670	0.0079	0.0021
	glass[c] (77)	563, 609 sh	3.96	
3	MeOH (298)	652	0.040	0.0065
	buffer[b] (298)	670	0.0084	0.0020
	glass[c] (77)	563, 608 sh	3.93	
4	MeOH (298)	605	0.087	0.020
	buffer[b] (298)	600	0.061	0.020
	glass[c] (77)	537, 570 sh	4.94	
5	CH_3CN (298)	632	0.10	0.015
	MeOH (298)	650	0.043	0.0058
	buffer[b] (298)	661	0.0078	[d]
	glass[c] (77)	563, 609 sh	3.95	

[a] Excitation wavelength = 350 nm. [b] 50 mM potassium phosphate buffer pH 7.4/MeOH (9:1, v/v). [c] EtOH/MeOH (4:1, v/v). [d] The quantum yield cannot be determined accurately because of insufficient solubility of the complex.

Luminescence Properties. Upon photoexcitation, all the complexes exhibited intense and long-lived greenish-yellow to red luminescence in fluid solutions under ambient conditions and in low-temperature glass. The photophysical data of all the complexes are summarized in Table 2. The emission spectra of complex **2** in CH_3CN and MeOH solutions at 298 K and in alcohol glass at 77 K are shown in Figure 2. The emission energies, quantum yields, and excited-state lifetimes of the complexes depend strongly on the diimine, and the observed order (**1** > **4** > **2** ≈ **3** ≈ **5**) is in accordance with the π-accepting properties of the bpy ligands. This suggests that the emission of the complexes is associated with a ^{3}MLCT (dπ (Ir) $\rightarrow \pi^*$ (N^N)) emissive state.[6,7,8a,8b,9b,9c,10,11,12a,12b,13,15b−15g,16−18,-19b−19d,20−24] The assignment of a ^{3}CT state has been supported by the significant blue-shifts of the emission maxima of all the complexes upon cooling from room temperature to 77 K. Importantly, the introduction of one or two electron-withdrawing amide group(s) to the bpy ligand of complex **1** has changed the yellow luminescence to orange (complex **4**) and red (complexes **2**, **3**, and **5**) in aqueous solutions. This reflects the facile

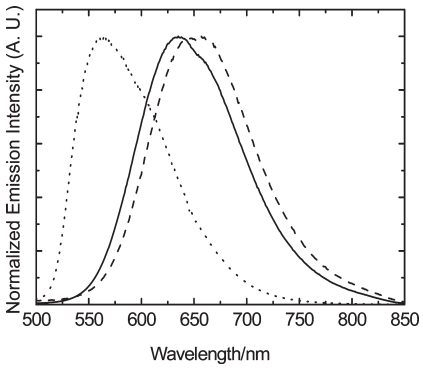

Figure 2. Emission spectra of complex **2** in CH_3CN (solid line) and MeOH (dashed line) at 298 K and in EtOH/MeOH (4:1, v/v) at 77 K (dotted line).

Table 3. Electrochemical Data of Complexes **1**−**5**[a]

complex	oxidation, $E_{1/2}$ or E_a/V	reduction, $E_{1/2}$ or E_c/V
1	+1.15,[b] +1.23[c]	−1.39, −2.06,[b] −2.30,[b] −2.64[b]
2	+1.29[c]	−1.07, −1.70,[c] −2.13,[b] −2.24,[b] −2.47[b]
3	+1.28[c]	−1.08, −1.64,[c] −2.12,[b] −2.24,[b] −2.48[b]
4	+1.10,[b] +1.21[c]	−1.29, −1.77,[b] −2.26,[b] −2.70[b]
5	+1.29[c]	−1.15, −1.71,[c] −2.19,[b] −2.48[b]

[a] In CH_3CN (0.1 M TBAP) at 298 K (glassy carbon working electrode, sweep rate = 100 mV s^{-1}, all potentials versus SCE). [b] Irreversible waves. [c] Quasi-reversible couples.

emission-color tunability of these iridium(III) polypyridine complexes, which is an attractive advantage in the development of multicolor luminescent biological probes.

Electrochemical Properties. The electrochemical properties of all the complexes have been studied by cyclic voltammetry. The electrochemical data are listed in Table 3. All the complexes showed a quasi-reversible couple at about +1.21 to +1.29 V versus SCE, which has been ascribed to the metal-centered iridium(IV/III) oxidation.[6c,7,8a,8b,9a,9b,10,11a,11c,12a,12b,13d,14,15b−15d,15g,16,17a,17b,19a−19c,20,21,24a,24c−24n,24r,24s] Complexes **1** and **4** exhibited an additional irreversible wave at +1.15 and +1.10 V, respectively, attributable to the oxidation of the secondary amines of the cyclometalating ligands.[24f,24l] The first reduction couples of all the complexes were reversible and appeared at about −1.07 to −1.39 V versus SCE. They have been assigned to the reduction of the bipyridine ligands.[7,10,11c,12a,12b,13d,15b−15d,15g,16,17a,17b,19a,20,24a,24c−24n,-24r,24s] This is in agreement with the facts that (1) the electron-withdrawing amide substituent of the bpy ligand rendered the reduction of complex **4** to occur at a less negative potential (−1.29 V) compared to that of the bpy complex **1** (−1.39 V); (2) complexes **2**, **3**, and **5**, all of which contain two amide substituents on their bpy ligands, revealed the least negative reduction potential (ca. −1.07 to −1.15 V). Additionally, the reduction waves at more negative potentials are irreversible, and have been assigned to the reduction of the bpy and the cyclometalating ligands.[7,10a−10c,10e,11c,12b,15b−15d,15g,16,17a,24a,24c−24n,24r,24s]

HABA Assays. The avidin-binding properties of the biotin complexes **1**−**4** have been studied by HABA assays, which are based on the competition between biotin and HABA on binding to the biotin-binding sites of avidin. The binding of HABA to avidin results in an absorption feature at about 500 nm.[4a] Since the binding

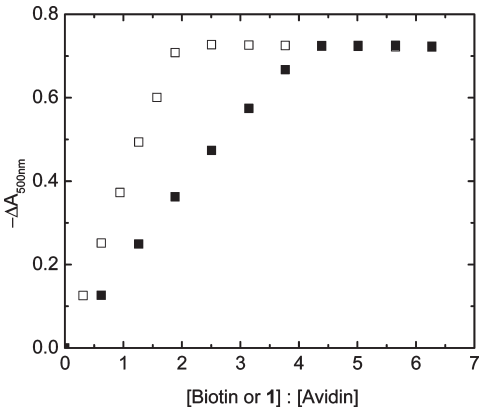

Figure 3. Results of spectrophotometric titrations of avidin-$(HABA)_4$ with unmodified biotin (■) and complex **1** (□).

of HABA to avidin (K_d = ca. 6×10^{-6} M) is much weaker than that of biotin (K_d = ca. 10^{-15} M),[1,4a] addition of biotin displaces the bound HABA molecules, leading to a decrease of the absorbance at 500 nm. Addition of complexes **1**−**4** to a mixture of avidin and HABA resulted in a decrease in absorbance at 500 nm, indicating the binding of the biotin moieties of the complexes to avidin. The results of spectrophotometric titrations of avidin-$(HABA)_4$ with unmodified biotin and complex **1**, respectively, are shown in Figure 3. If the biotin moieties of the complexes can displace the avidin-bound HABA molecules, the equivalence points should occur at [Ir]:[avidin] = 2 and 4/3 for the bis- and tris-biotin complexes, respectively. We found that complexes **1**−**3** showed an equivalence point at [Ir]:[avidin] = 2.0. However, the equivalence point for complex **4** appeared at [Ir]:[avidin] = about 1.6, which is larger than the ideal value 4/3. This suggests that the binding is not sufficiently strong and/or not all three biotin moieties of the complex are functional simultaneously because of steric hindrance.

Emission Titrations. The avidin-binding properties of the biotin complexes **1**−**4** have been investigated by emission titrations of avidin using the complexes as the titrants. The titration results have been compared to two control experiments in which (i) avidin was absent, and (ii) avidin was presaturated with excess unmodified biotin. The titration curves of complexes **1**−**4** are shown in Figure 4. Similar to our previous studies,[24f,24h−24j,24l,24m,24o,24q] all the complexes displayed higher emission intensities (1.3 to 2.5-fold) and longer lifetimes (1.2 to 1.5-fold) in the presence of avidin (Table 4). These findings result from the binding of the biotin moieties of the complexes to the biotin-binding sites of avidin as evidenced by the lack of changes in the control experiments. The observed changes have been attributed to the increase of hydrophobicity and rigidity of the local environment of the complexes after they bind to avidin, which is in agreement with the emission data of the complexes in solvents of different polarity (Table 2). It is interesting to note that among the complexes studied here, complex **1** showed the smallest avidin-induced emission enhancement (I/I_o = 1.3), which is comparable to the that of the bis-biotin complexes $[Ir(ppyC6B)_2(N^\wedge N)](PF_6)$ ($N^\wedge N$ = 3,4,7,8-tetramethyl-1,10-phenanthroline, Me_4-phen; 4,7-diphenyl-1,10-phenanthroline, Ph_2-phen) (I/I_o = 1.6 and 1.2, respectively).[24l] Complexes **2** and **3**, in which the two biotin moieties

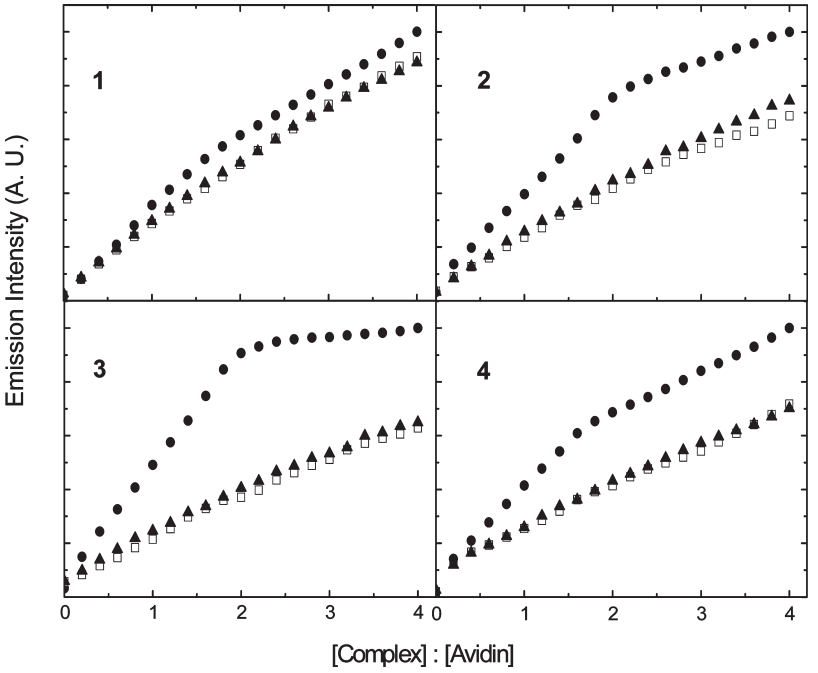

Figure 4. Emission titration curves for the titrations of (i) 10 μM avidin (●), (ii) 10 μM avidin and 1 mM unmodified biotin (▲), and (iii) a blank phosphate buffer solution (□) with complexes **1**−**4**.

Table 4. Relative Emission Intensities and Emission Lifetimes of the Biotin Complexes **1**−**4** in the Absence and Presence of Avidin (and Excess Biotin) in Aerated 50 mM Potassium Phosphate Buffer pH 7.4/MeOH (9:1, v/v) at 298 K

complex[a]	I (τ/ns)[b]	I (τ/ns)[c]	I (τ/ns)[d]
1	1.00 (190)	1.32 (230)	1.00 (190)
2	1.00 (7.8)	1.81 (9.9)	1.07 (7.9)
3	1.00 (7.4)	2.45 (9.7)	1.09 (7.4)
4[e]	1.00 (30)	1.79 (44)	1.02 (31)

[a] [Ir] = 20 μM. [b] [avidin] = 0 M, [biotin] = 0 M. [c] [avidin] = 10 μM, [biotin] = 0 M. [d] [avidin] = 10 μM, [biotin] = 1 mM. [e] [Ir] = 16 μM.

are appended to the bpy ligand, exhibited larger emission enhancement factors (1.8−2.5). Thus, it appears that the two biotin units on the same bpy ligand can lead to a higher degree of rigidity upon binding of the complexes to avidin. The equivalence points of the titrations occurred at [Ir]:[avidin] = about 2.0 and 1.6 for the bis-biotin complexes **1**− **3** and the tris-biotin complex **4**, respectively (Figure 4), indicating that the two or three biotin moieties of the same complex can bind to avidin. However, results of the HABA assays and emission titrations do not provide information on whether the binding is intermolecular or intramolecular with respect to avidin.

Dissociation Assays. The stability of the avidin-adducts of the biotin complexes **1**−**4** has been examined by dissociation assays. In these assays, dissociation of the avidin-bound iridium(III) biotin complex was induced by addition of excess unmodified biotin, and the emission intensity was measured. Among the complexes, complex **1** showed the largest off-rate constant k_{off} (6.5×10^{-3} s^{-1}) (Table 5), reflecting the lowest stability of the **1**-avidin adduct and the weaker binding affinity of the biotin moieties on the cyclometalating ligands. The k_{off} values of complexes **2** and **3** are very similar (ca. 2.0×10^{-4} s^{-1}) and about 30-fold smaller than that of complex **1** (Table 5). This much higher stability of the **2**-avidin and **3**-avidin adducts suggests the stronger avidin-binding

Table 5. Rate Constants for the Dissociation of the Avidin-Bound Biotin Complexes **1**−**4** in 50 mM Potassium Phosphate Buffer pH 7.4/MeOH (9:1, v/v) at 298 K

complex[a]	k_{off}/s^{-1}
1	6.5×10^{-3}
2	2.0×10^{-4}
3	2.0×10^{-4}
4[b]	3.6×10^{-4}

[a] [Ir] = 20 μM, [avidin] = 10 μM, [biotin] = 2 mM. [b] [avidin] = 12.5 μM.

affinity of the biotin units on the bpy ligands. Interestingly, the k_{off} value of the tris-biotin complex **4** (3.6×10^{-4} s^{-1}) is larger than those of complexes **2** and **3**, indicating that the **4**-avidin adduct is even less stable than the avidin-adducts of the bis-biotin complexes **2** and **3**. This observation is in accordance with the fact that two of the three biotin groups are connected to the cyclometalating ligands, which appears to show weaker avidin-binding.

Microsphere Assays for Avidin-Cross-Linking Properties. The avidin-cross-linking properties of the biotin complexes **1**−**4** have been studied by an assay involving green-fluorescent microspheres that have been conjugated with avidin. An iridium(III) monobiotin complex [Ir(ppy)$_2$(bpyC2B)](PF$_6$) (bpyC2B = 4-(*N*-((2-biotinamido)ethyl)aminomethyl)-4′-methyl-2,2′-bipyridine)[24f] was used for comparison. The confocal microscopy images of the fluorescent avidin-conjugated microsphere suspensions that have been incubated with [Ir(ppy)$_2$(bpyC2B)](PF$_6$) and complexes **1**−**4**, respectively, are shown in Figure 5, panels (a)−(e). The observed emission originated from the dye entrapped in the microspheres instead of the complexes because the emission of the complexes at the wavelength monitored (505 nm) is weak and totally masked by the strong green fluorescence of the microspheres. Agglomeration of avidin-modified microspheres occurred in the cases of the biotin complexes **1**−**4**

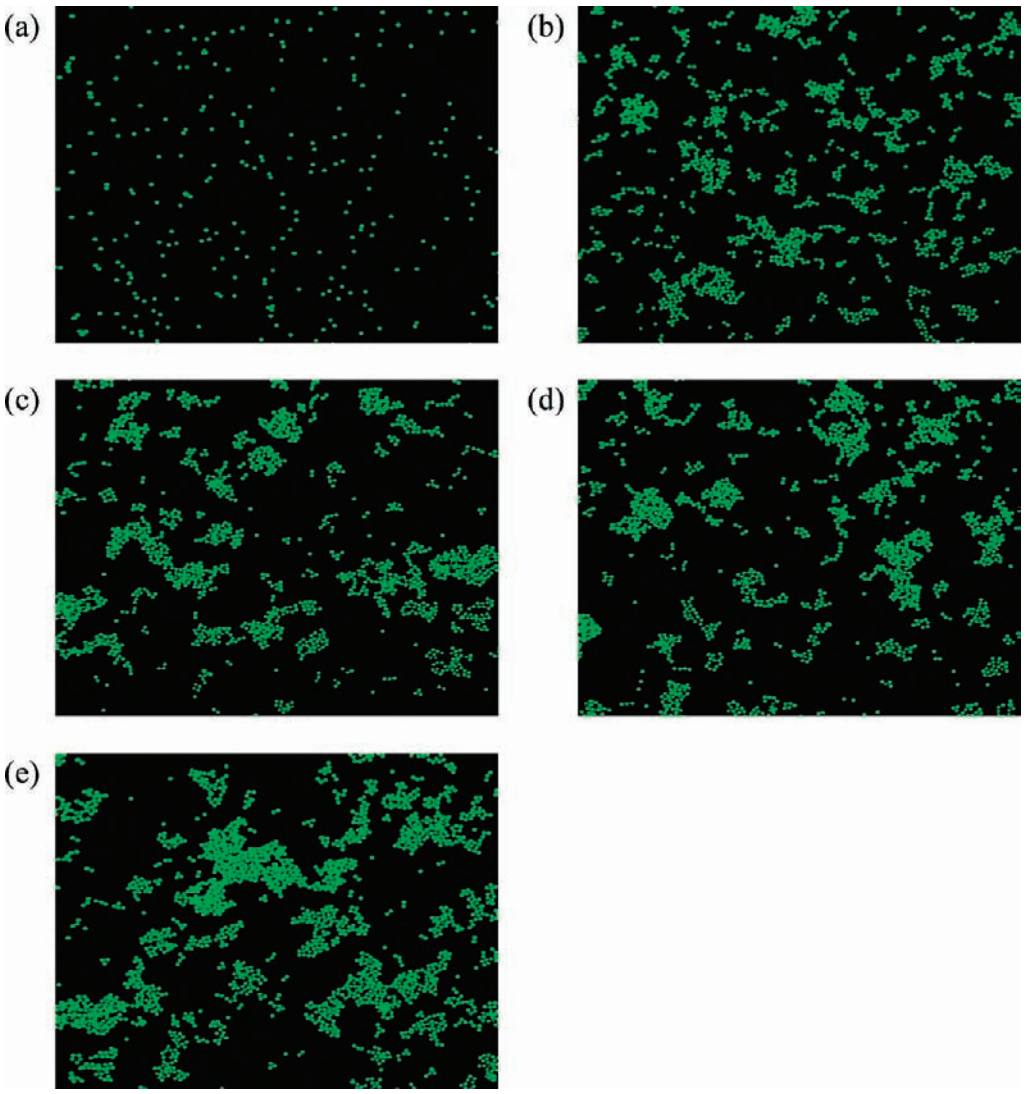

Figure 5. Confocal microscopy images of green fluorescent microsphere sample suspensions containing (a) $[Ir(ppy)_2(bpyC2B)](PF_6)$, (b) complex **1**, (c) complex **2**, (d) complex **3**, and (e) complex **4**.

(Figure 5, panels (b)−(e)). This has been attributed to the cross-linking of avidin molecules on different microspheres instead of nonspecific interactions because similar aggregation did not occur (1) when excess biotin was present in the reaction mixtures from the outset and (2) in the case of the monobiotin complex $[Ir(ppy)_2(bpyC2B)](PF_6)$ (Figure 5(a)). The images revealed that the degree of microsphere aggregation is similar among the bis-biotin complexes **1**−**3** but appears to be higher for the tris-biotin complex **4** (Figure 5(e)).

HPLC Analysis for Avidin-Cross-Linking Properties. Size-exclusion HPLC experiments have been performed to further understand the avidin-cross-linking properties of the biotin complexes **1**−**4**. Under the chromatographic conditions we employed, avidin was eluted at 12.5 min (Figure 6(a)). Chromatograms of an equimolar mixture of avidin and the monobiotin complex $[Ir(ppy)_2(bpyC2B)](PF_6)$,[24f] bis-biotin complex **1**, and tris-biotin complex **4** are shown in Figure 6, panels (b)−(d), respectively. It can be seen that the presence of $[Ir(ppy)_2(bpyC2B)](PF_6)$ in a solution of avidin caused a small increase in the retention time of the protein to about 13.0 min, and some band broadening was observed, which could be due to increased hydrophobicity of the adduct. Interestingly, addition of the bis-biotin complex **1** to a solution of avidin resulted in the appearance of a shoulder at about 9.1 min and two new bands at about 10.0 and 11.1 min ($I_{9.1\ min}$:$I_{10.0\ min}$:$I_{11.1\ min}$:$I_{13.0\ min}$ = ca. 0.2:0.4:0.6:1.0) (Figure 6(c)). With reference to previous chromatographic work of oligomeric streptavidin molecules,[5a] we have assigned these new features at about 9.1, 10.0, and 11.1 min to avidin tetramer, trimer, and dimer, respectively. Remarkably, when the tris-biotin complex **4** was used, these bands were much higher in intensity ($I_{9.1\ min}$:$I_{10.0\ min}$:$I_{11.1\ min}$:$I_{13.0\ min}$ = ca. 0.8:0.8:0.9:1.0; Figure 6(d)) and an additional shoulder at about 8.4 min, which is likely to be due to avidin oligomers or polymers, was observed.[5a] These chromatographic results show that bis- and tris-biotin complexes can cross-link avidin molecules, and the efficiency is higher for the tris-biotin complex, which is in agreement with the results of the microsphere assays. The relative peak heights reveal that the cross-linking efficiency of the complexes in this work is higher than that of other related iridium(III) bis-biotin complexes $[Ir(ppyC6B)_2(N^\wedge N)](PF_6)$ ($N^\wedge N$ = Me_4-phen, Ph_2-phen).[24l]

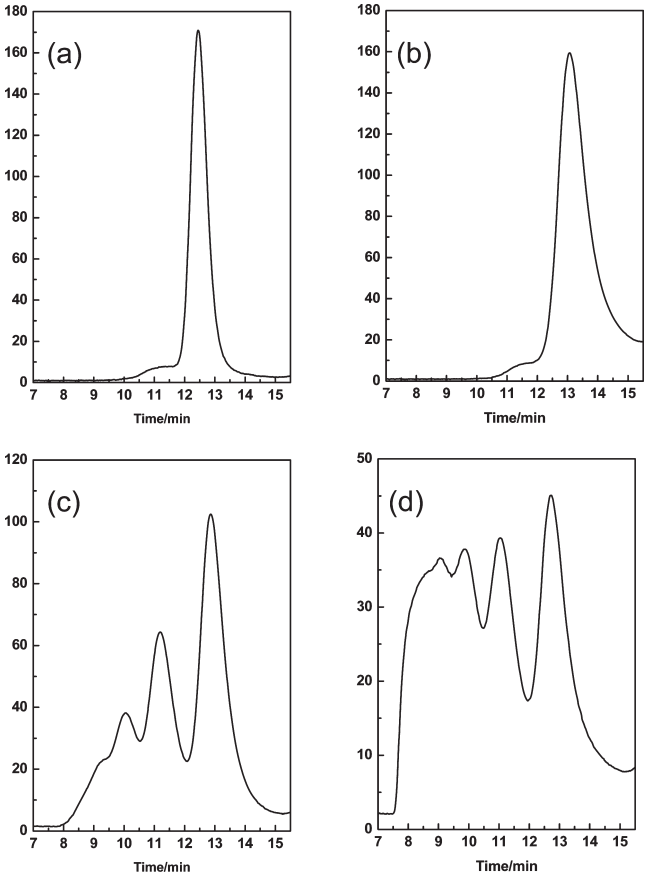

Figure 6. Size-exclusion chromatograms of (a) 0.12 mM avidin, and an equimolar mixture of 0.12 mM avidin and (b) the monobiotin complex $[Ir(ppy)_2(bpyC2B)](PF_6)$, (c) bis-biotin complex **1**, and (d) tris-biotin complex **4**, respectively, in 50 mM potassium phosphate buffer pH 7.4. The broad signals at about 11.3 min in (a) and (b) are due to impurity or nonspecific protein aggregates.

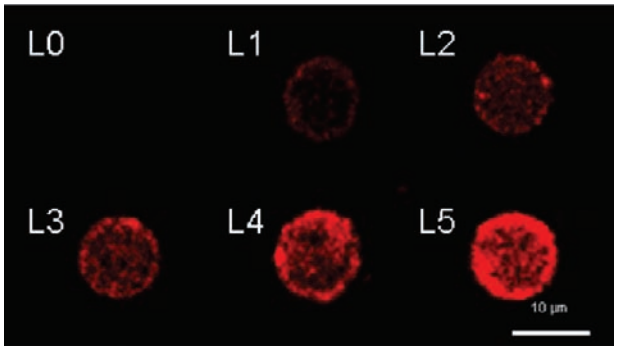

Figure 7. Confocal microscopy images of avidin-coated nonfluorescent microspheres upon immobilization of zero (L0), one (L1), two (L2), three (L3), four (L4), and five (L5) layers of complex **3**.

Signal Amplification Studies. One of the objectives of this work is the exploration of the bifunctional (luminescence and avidin-cross-linking) properties of the iridium (III) multiple-biotin complexes in emission signal amplification for the detection of biotinylated molecules. As an example, successive incubation of avidin-coated nonfluorescent microspheres with complex **3** was performed, with stringent washing between each incubation step. The confocal microscopy images of typical microspheres upon immobilization of zero to five layers of complex **3** are shown in Figure 7. We found that the microsphere samples acquired increasing emission intensities upon successive immobilization of complex **3** (Figures 7 and 8). After immobilization of five layers of the complex, the average emission intensity of the microspheres was about 18 times higher than those immobilized with just one layer of complex. Similar results were not obtained when BSA was used instead of avidin or when the avidin was presaturated with biotin from the outset (Figure 8), indicating that the increasing emission intensity relies on the emission and avidin-cross-linking properties of complex **3**. We anticipate that this interesting emission signal amplification can be applied in heterogeneous assays for a wide range of biological interactions such as antigen/hapten−antibody recognition and DNA hybridization.

Lipophilicity. The ability of a cellular probe and reagent to permeate biological membranes is closely related to its lipophilicity.[25] The lipophilicity of a compound is commonly estimated by the partition coefficient ($P_{o/w}$) in *n*-octanol/water.[26] The lipophilicity (log $P_{o/w}$ values) of all the complexes in this work has been determined by reversed-phase HPLC, and the results are listed in Table 6. Incorporation of two C6-biotin units into the ppy ligands of $[Ir(ppy)_2(bpy)](PF_6)$ increased the lipophilicity from 1.12[24n] to 1.34 (complex **1**). Since biotin is relatively polar, this increase should originate from the two aliphatic C6 spacer-arms. Changing the bpy ligand of complex **1** to the bpyC6B ligand further increases the lipophilicity to 1.91 (complex **4**). The increase was brought about by the methyl group and C6 spacer-arm on the bpy ligand of complex **4**. It is noteworthy that complex **2**, which possesses two C2-biotin moieties on the bpy ligand, showed much higher lipophilicity (2.36) than $[Ir(ppy)_2(bpy)](PF_6)$ (1.12).[24n] Also, extension of the C2 spacer-arms of complex **2** (log $P_{o/w}$ = 2.36) with an additional C6 unit results in an increase of lipophilicity to 2.83 (complex **3**). It is important to point out that the biotin-free complex **5** exhibited the highest lipophilicity among all the complexes, reflecting the hydrophobicity of the diimine ligand bpyC4 and the polar nature of biotin.

Cytotoxicity. The cytotoxicity of all the complexes toward the HeLa cell line has been studied by MTT assays,[27] in which the dose dependence of surviving cells after exposure to the complexes for 48 h has been evaluated. Although the IC_{50} values of the biotin complexes **1**−**4** could not be determined because of limited solubility of the complexes in aqueous solution, these complexes are basically noncytotoxic (IC_{50} values >400 μM). In contrast, the biotin-free complex **5** exhibited a relatively low IC_{50} value (3.2 ± 0.4 μM), which is almost 9 times smaller than that of cisplatin (27.9 ± 3.0 μM) under the same experimental conditions. The lower cytotoxicity of the biotin complexes **1**−**4** could be related to the presence of biotin moieties and/or the lower lipophilicity of these complexes. The cytotoxicity of complex **5** is comparable to other cyclometalated iridium(III) polypyridine indole complexes (1.1 to 6.3 μM)[24s] and their structural analogues (3.8 to 18.1 μM).[24r] However, in general, the cytotoxicity of complex **5** is slightly higher than that of the

(25) VanBrocklin, H. F.; Liu, A.; Welch, M. J.; O'Neil, J. P.; Katzenellenbogen, J. A. *Steroids* **1994**, *59*, 34–45.
(26) Minick, D. J.; Frenz, J. H.; Patrick, M. A.; Brent, D. A. *J. Med. Chem.* **1988**, *31*, 1923–1933.
(27) Mosmann, T. *J. Immunol. Methods* **1983**, *65*, 55–63.

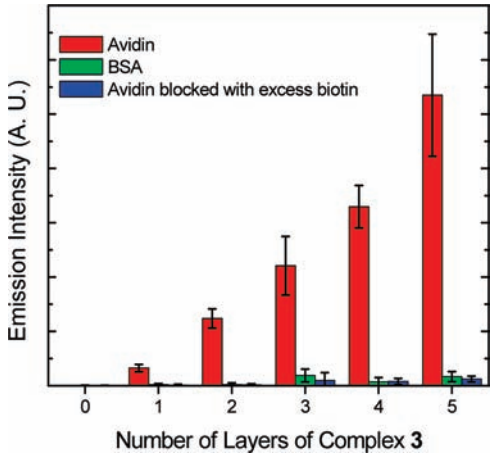

Figure 8. Averaged emission intensities of avidin-modified nonfluorescent microspheres ($N = 10$) upon incubation of zero to five layers of complex **3**. Results of the control experiments (BSA was used instead of avidin or the avidin was presaturated with biotin from the outset) are included.

Table 6. Lipophilicity (log $P_{o/w}$) of Complexes **1**−**5** and $[Ir(ppy)_2(bpy)](PF_6)$

complex	log $P_{o/w}$
1	1.34
2	2.36
3	2.83
4	1.91
5	3.40
$[Ir(ppy)_2(bpy)](PF_6)$	1.12[a]

[a] From reference 24n.

rhenium(I) diphosphine complexes $[Re(CO)_3(diphosphine)Br]$[28a] and much higher than that of $[Re(CO)_3(2\text{-appt})Cl]$ (2-appt = 2-amino-4-phenylamino-6-(2-pyridyl)-1,3,5-triazine) (IC_{50} = ca. 50 μM) and $[Ru(^tBu_2\text{-bpy})_2(2\text{-appt})]^{2+}$ ($^tBu_2$-bpy = 4,4′-di-*tert*-butyl-2,2′-bipyridine) (IC_{50} = 59.7 μM), both of which bind to the minor groove of double-stranded DNA.[28b] Complex **5** is relatively cytotoxic compared to the organometallic ruthenium arene complexes $[(\eta^6\text{-arene})Ru(ethylenediamine)(X)](PF_6)_n$ (X = substituted pyridines and halides), some of which exhibit fast hydrolysis kinetics and high cytotoxicity toward the human ovarian cancer cell line A2780.[28c]

Cellular Uptake Studies. The amounts and concentrations of iridium associated with HeLa cells incubated with the complexes (5 μM, at 37 °C for 3 h) were determined by ICP-MS measurements. We found that an average cell (mean volume of 3.4 pL) contained 2.3×10^{-16} to 5.8×10^{-15} mol of iridium (Table 7), which is comparable to those reported in the cellular uptake studies of other inorganic complexes.[29−31] Whereas the concentrations of the biotin complexes **1**−**4** ranged from 67 to 94 μM,

Table 7. Numbers of Moles and Concentrations of Iridium Associated with an Average HeLa Cell upon Incubation with Complexes **1**−**5** (5 μM) at 37 °C for 3 h Determined by ICP-MS

complex	number of moles	concentration/μM
1	3.1×10^{-16}	90
2	3.2×10^{-16}	94
3	2.4×10^{-16}	70
4	2.3×10^{-16}	67
5	5.8×10^{-15}	1700

the biotin-free complex **5** displayed a much higher cellular uptake level ([Ir] = 1.7 mM). These findings point to the fact that the cellular uptake efficiencies of the complexes are closely related to their lipophilicity of the complexes, although we cannot exclude the possibility that the highest cellular uptake of complex **5** may also be a result of its smallest molecular size. Nevertheless, it is important to note that the iridium concentrations of all the complexes are much higher than that in the medium (5 μM), indicating that the complexes were concentrated within the cells. However, strictly speaking, the measured concentrations indicate iridium associated with the cells, which is not necessarily in the interior. Thus, the data can only serve as an approximate indicator for cellular uptake efficiencies.

Live-Cell Confocal Imaging and Flow Cytometry. In view of the interesting luminescence properties of complexes **1**−**5**, the possibility of using these complexes as imaging reagents for live cells has been investigated using laser-scanning confocal microscopy. The microscopy images of HeLa cells treated with complexes **1**−**5** (5 μM) for 3 h are illustrated in Figure 9. The emission intensities of cells loaded with the biotin complexes **1**−**4** are considerably weaker than that of the biotin-free complex **5**. This should be related to the much lower cellular uptake efficiency of the biotin complexes (Table 7) because the emission intensity of free complex **5** in buffer solution is actually the weakest among the complexes (Table 2). We have studied the cellular uptake of the avidin adducts of complexes **1**−**4**, and the confocal images were similar to those of the free complexes. In general, HeLa cells treated with all the free complexes showed punctate cytoplasmic staining with much weaker or no emission from the nuclei, indicative of negligible nuclear uptake (Figure 9). In the cases of complexes **1**−**4**, emissive cytoplasmic granules were observed, which may result from endosomal labeling and/or aggregation of the luminescent complexes after cellular internalization.[32] Importantly, HeLa cells loaded with complex **5** revealed much more intense emission. It is interesting to note that, upon cellular uptake, this complex formed a diffuse background in addition to cytoplasmic granules that were also observed in the other four complexes (Figure 9).

Since complex **5** gave the brightest images, its cellular uptake properties have been studied in more detail by flow cytometry and confocal microscopy. Flow cytometric results indicated that incubation of HeLa cells with this complex at 4 °C resulted in lower uptake efficiency (Figure 10(a)). Interestingly, the confocal microscopy images only displayed a diffuse background as observed at 37 °C, and the cytoplasmic foci disappeared (Figure 11(a)). This suggests that the complex enters the cells by two mechanisms: (1) an energy-dependent, endocytosis-like pathway that gave rise to the cytoplasmic

(28) (a) Zhang, J.; Vittal, J. J.; Henderson, W.; Wheaton, J. R.; Hall, I. H.; Hor, T. S. A.; Yan, Y.-K. *J. Organomet. Chem.* **2002**, *650*, 123–132. (b) Ma, D.-L.; Che, C.-M.; Siu, F.-M.; Yang, M.; Wong, K.-Y. *Inorg. Chem.* **2007**, *46*, 740–749. (c) Wang, F.; Habtemariam, A.; van der Geer, E. P. L.; Fernández, R.; Melchart, M.; Deeth, R. J.; Aird, R.; Guichard, S.; Fabbiani, F. P. A.; Lozano-Casal, P.; Oswald, I. D. H.; Jodrell, D. I.; Parsons, S.; Sadler, P. J. *Proc. Natl. Acad. Sci. U.S.A.* **2005**, *102*, 18269–18274.
(29) Brunner, J.; Barton, J. K. *Biochemistry* **2006**, *45*, 12295–12302.
(30) Yu, J.; Parker, D.; Pal, R.; Poole, R. A.; Cann, M. J. *J. Am. Chem. Soc.* **2006**, *128*, 2294–2299.
(31) Chauvin, A.-S.; Comby, S.; Song, B.; Vandevyver, C. D. B.; Bünzli, J.-C. G. *Chem.—Eur. J.* **2008**, *14*, 1726–1739.

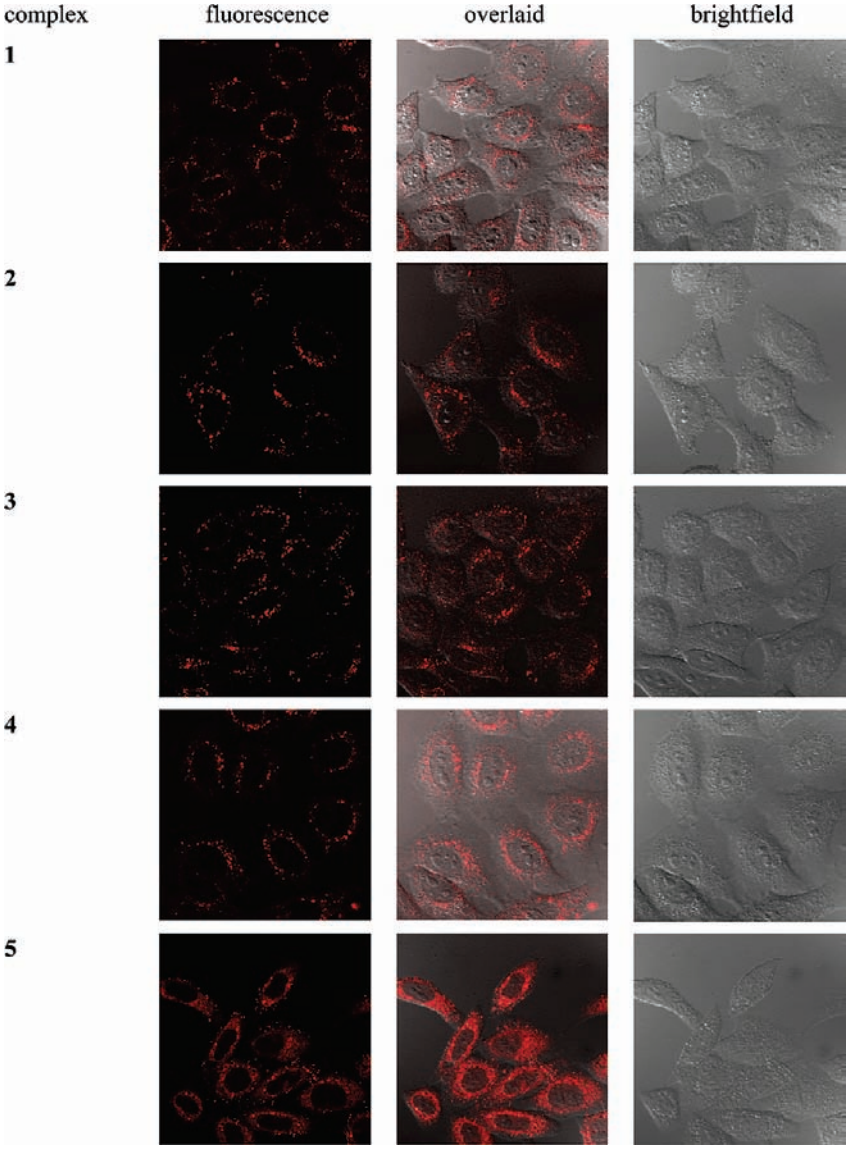

Figure 9. Microscopy images of HeLa cells incubated with complexes **1**−**5** (5 μM) at 37 °C for 3 h.

granules, and (2) an energy-independent diffusion-like pathway that led to a more diffuse background.[32] The effects of different reagents including cytoskeletal-, metabolic-, and ATPase-inhibitors on the cellular uptake of complex **5** have been investigated.[33] First, we treated HeLa cells with colchicine (10 μM), which is a typical cytoskeletal inhibitor that disrupts the microtubule assembly,[33] before adding complex **5**. Although the loaded HeLa cells showed a similar emission intensity regardless if they have been pretreated with colchicine or not (Figure 10(b)), the luminescence images are noticeably different in that the distribution of the complex was more even, with a diffuse background, in the *whole* of the cytoplasm. More apparently, cytoplasmic foci were not observed in these cells (Figure 11(b)). Since the disruption of tubulin inhibits endocytosis, these images are supportive of the endocytic uptake, as well as the passive-diffusion pathways of the complex. This result also highlights the important role of cytoskeleton in the intracellular transport of complex **5**. Second, incubation of HeLa cells with carbonyl cyanide 3-chlorophenylhydrazone (CCCP) (20 μM), a metabolic inhibitor,[33] at 37 °C in a glucose-free medium before treatment with complex **5** led to a substantial decrease of cellular uptake efficiency (Figures 10(c) and 11(c)). Since CCCP inhibits oxidative phosphorylation, resulting in decreased ATP production and hence a lowered metabolic rate, the observed decrease of cellular uptake is in accordance with the argument that internalization of complex **5** occurred, to a certain extent, via energy-requiring endocytosis. Additionally, the ATPase inhibitor potassium nitrate (50 mM) did not result in any significant changes in the cellular uptake and intracellular migration and distribution of complex **5** (Figures 10(d) and 11(d)).[33] Remarkbly, incubation of HeLa cells with *N*-ethylmaleimide (NEM) (0.1 mM) for 20 min followed by washing and treatment

(32) (a) Kobayashi, T.; Arakawa, Y. *J. Cell Biol.* **1991**, *113*, 235–244. (b) Pagano, R. E.; Martin, O. C.; Kang, H.-C.; Haugland, R. P. *J. Cell Biol.* **1991**, *113*, 1267–1279. (c) Haugland, R. P. *The Handbooks - A Guide to Fluorescent Probes and Labeling Technologies*, 10th ed.; Molecular Probes, Inc.: Eugene, OR, 2005; Section 12. See http://probes.invitrogen.com/handbook/sections/1200.html.

(33) Reaven, E.; Tsai, L.; Azhar, S. *J. Biol. Chem.* **1996**, *271*, 16208–16217.

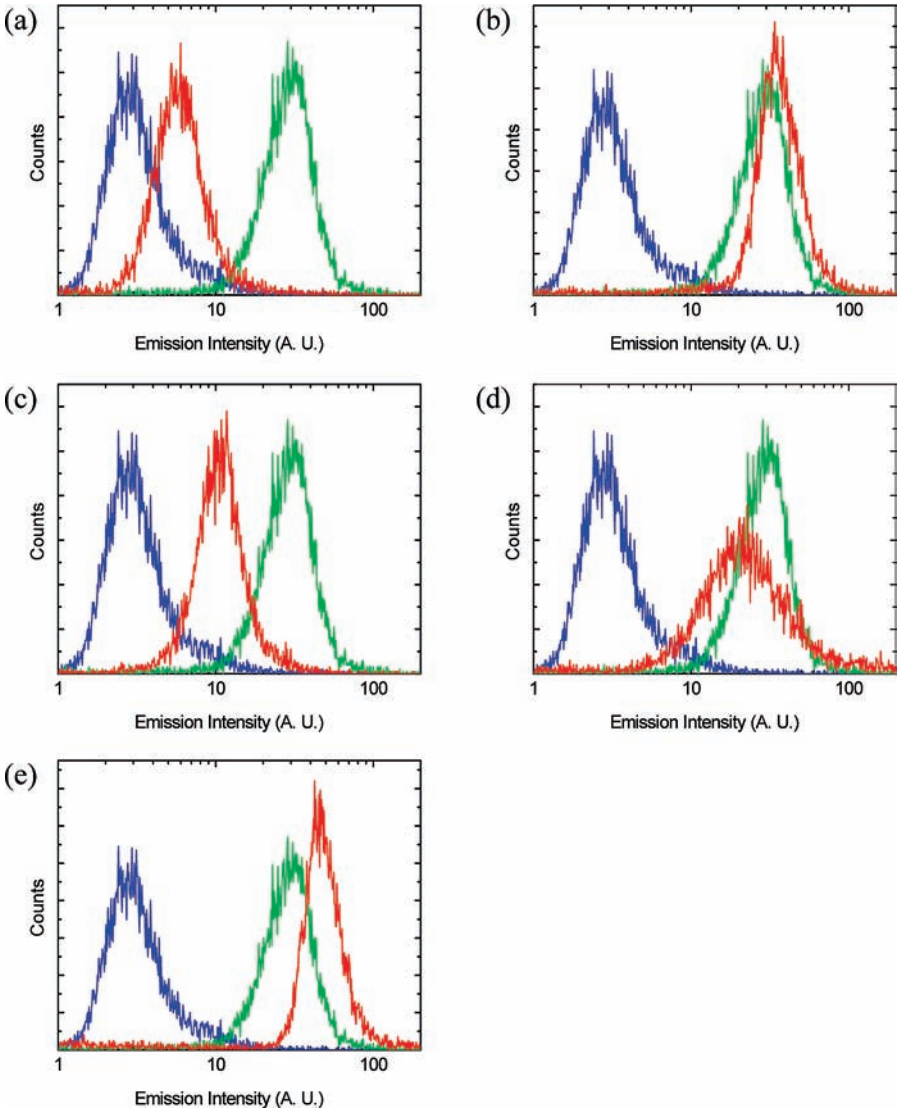

Figure 10. Flow cytometric results of HeLa cells incubated with blank medium (blue) and complex **5** (green) at 37 °C and after the cells were preincubated (red) (a) at 4 °C, or with (b) colchicine (10 μM), (c) CCCP (20 μM), (d) potassium nitrate (50 mM), and (e) NEM (0.1 mM).

with complex **5** (5 μM) for 1 h resulted in significant cytoplasmic and nuclear staining (Figures 10(e) and 11(e)), and the cell morphology and the presence of intracellular vacuoles revealed a mild degree of cell death. A similar finding was obtained when the cells were loaded with the complex prior to incubation with NEM (0.1 mM) for 20 min (data not shown). Interestingly, propidium iodide staining experiments indicated that cells treated with NEM only, under the same conditions, remained viable. This cell death as a result of the treatment with both complex **5** and NEM could originate from nuclear uptake of the complex. Nuclear accumulation of the complex can possibly be caused by an increased nuclear entry as a result of NEM-induced nuclear pore malformation, or a reduced nuclear export because of the inhibitory effect of NEM on nuclear export pathways.[34] Importantly, HeLa cells fixed with MeOH before treatment with the complex revealed similar staining in the cytoplasm and nucleus (Figure 11(f)), which is in agreement with that the complex can accumulate in the nucleus with a compromised membrane.

Conclusions

In this work, luminescent iridium(III) bis- and tris-biotin complexes and their biotin-free counterpart have been synthesized and characterized. The photophysical and electrochemical properties of these complexes have been investigated. The emission energy, quantum yields, excited-state lifetimes, and the redox properties highly depend on the π-accepting properties of the bpy ligands. The interactions of the biotin complexes with avidin have been studied by assays and emission titrations. All the biotin complexes displayed higher emission intensities and longer lifetimes upon binding to avidin. The avidin-cross-linking properties have been examined by microscopy studies and HPLC analysis. Amplification of emission signals in heterogeneous assays has also been demonstrated using one of the bis-biotin complexes. Additionally, the cytotoxicity and cellular uptake properties of all the complexes have been examined using MTT assays, ICP-MS, and laser-scanning confocal microscopy, and the intracellular distribution of complex **5**

(34) Macaulay, C.; Forbes, D. J. *J. Cell Biol.* **1996**, *132*, 5–20.

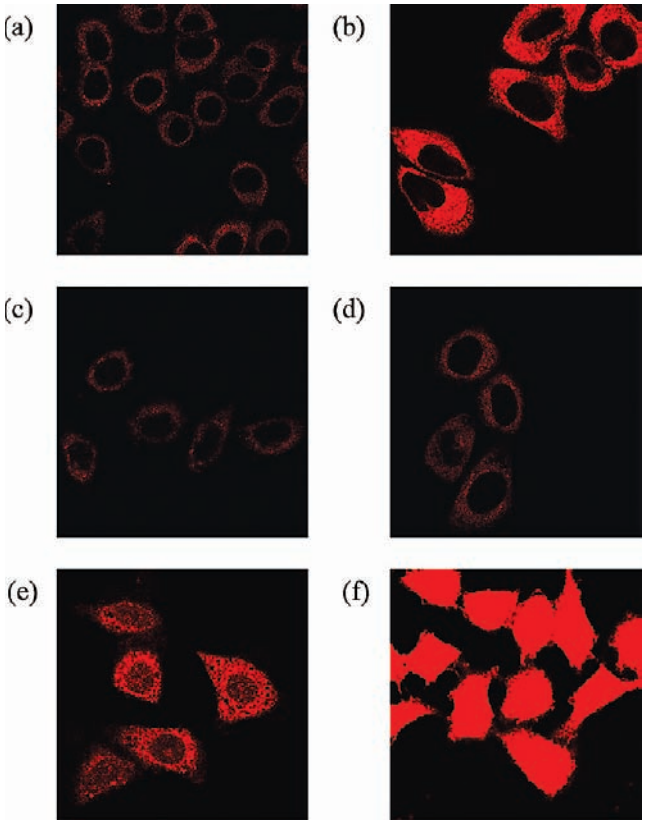

Figure 11. Confocal microscopy images of HeLa cells incubated with complex **5** (a) at 4 °C, and at 37 °C after the cells were preincubated with (b) colchicine (10 μM), (c) CCCP (20 μM), (d) potassium nitrate (50 mM), and (e) NEM (0.1 mM). (f) HeLa cells fixed with MeOH before treatment with complex **5**.

has also been studied in more detail using various inhibitors. We anticipate that these new reagents with interesting bifunctional properties (luminescence and avidin-cross-linking) will be useful in the studies of biological interactions such as antigen/hapten−antibody recognition and DNA hybridization, and in the development of new transition metal-based live-cell imaging agents.

Experimental Section

Materials and Synthesis. All solvents were of analytical reagent grade and purified according to standard procedures.[35] All buffer components were of biological grade and used as received. $IrCl_3 \cdot 3H_2O$, Hppy, Hpba, bpy, 4,4′-dimethyl-2,2′-bipyridine, *N*-Boc-1,6-diaminohexane hydrochloride, tetra-*n*-butylammonium hexafluorophosphate (TBAP), 1-octanol, 4-methoxyaniline, 4-methoxyphenol, phenol, acetophenone, naphthalene, *tert*-butylbenzene, anthracene, and pyrene were purchased from Aldrich. *N*-hydroxysuccinimide, *N*,*N*′-dicyclohexylcarbodiimide, chromium(VI) oxide, ethylenediamine, triethylamine, *n*-butylamine, $NaBH_4$, KPF_6, biotin, 1-(3-dimethylaminopropyl)-3-ethylcarbodiimide hydrochloride (EDC), cisplatin, colchicine, CCCP, potassium nitrate, and NEM were purchased from Acros. HABA and MTT were purchased from Sigma. Avidin was purchased from Calbiochem. 4-Succinimidyl-carboxy-4′-methyl-2,2′-bipyridine,[36] biotinyl-*N*-hydroxysuccinimidyl ester,[37] *N*-biotinyl-1,6-diaminohexane,[38] 6-biotinamidohexanoic acid *N*-hydroxysuccinimidyl ester,[37] bpy-C6B,[24h] and the precursor complexes $[Ir_2(pba)_4Cl_2]$,[24c] $[Ir_2(ppy)_4Cl_2]$,[39] and $[Ir(pba)_2(bpy)](PF_6)$[24c] were prepared according to reported procedures. Green fluorescent and nonfluorescent microspheres, both modified with carboxyl groups, were supplied by Bangs Laboratories. Tetra-*n*-butylammonium hexafluorophosphate was obtained from Aldrich and was recrystallized from hot ethanol and dried in vacuo at 110 °C before use. HeLa cells were obtained from American Type Culture Collection. Dulbecco's modified Eagle's medium (DMEM), fetal bovine serum (FBS), phosphate buffered saline (PBS), trypsin-EDTA, propidium iodide, and penicillin/streptomycin were purchased from Invitrogen. Unless specified, the growth medium for cell culture contained DMEM with 10% FBS and 1% penicillin/streptomycin.

4,4′-Dicarboxyl-2,2′-bipyridine, Bpy(COOH)$_2$. Concentrated sulfuric acid (25 mL) was slowly added to a solid sample of 4,4′-dimethyl-2,2′-bipyridine (1.11 g, 6.02 mmol) in a round-bottom flast in an ice−water bath. Chromium(VI) oxide (3.60 g, 36.00 mmol) was added to the mixture with vigorous stirring. The resulting mixture was refluxed until a clear green solution was obtained. Then, the solution was stirred at room temperature for 12 h. The green solution was poured over ice, and the white precipitate formed was collected by filtration and thoroughly washed with water, MeOH, and water, and dried in vacuo. The product was insoluble in common organic solvents and was used without further purification. Yield: 1.02 g (69%).

4,4′-Dimethoxycarbonyl-2,2′-bipyridine, Bpy(COOMe)$_2$. Concentrated sulfuric acid (10 mL) was added to a suspension of bpy(COOH)$_2$ (0.98 g, 4.01 mmol) in MeOH (80 mL). The mixture was refluxed for 12 h. Then H_2O (20 mL) was added to the mixture, and the suspension was neutralized with $NaHCO_3$. The aqueous solution was extracted with chloroform (15 mL × 3). The organic layer was dried over anhydrous $MgSO_4$ and evaporated to dryness to give bpy(COOMe)$_2$ as a white solid. Yield: 0.90 g (82%). Positive-ion ESI-MS ion clusters at m/z 273 $\{M + H^+\}^+$.

4,4′-Bis((2-aminoethyl)aminocarbonyl)-2,2′-bipyridine, Bpy(COen)$_2$. A mixture of bpy(COOMe)$_2$ (0.80 mg, 2.94 mmol) and ethylenediamine (5.0 mL, 74 mmol) in CH_2Cl_2 (50 mL) was stirred under an inert atmosphere of nitrogen at room temperature for 12 h. A copius amount of white precipitate was formed. The suspension was evaporated to dryness to give a yellow solid. The solid was washed with CH_2Cl_2, cold MeOH, and diethyl ether. The product was dried in vacuo and collected as a white solid. Yield: 0.95 g (98%). Positive-ion ESI-MS ion clusters at m/z 329 $\{M + H^+\}^+$.

BpyC2B2. A mixture of bpy(COen)$_2$ (150 mg, 0.46 mmol) and biotinyl-*N*-hydroxysuccinimidyl ester[37] (631 mg, 1.84 mmol) in DMF (200 mL) and triethylamine (1 mL) was heated at 80 °C under an inert atmosphere of nitrogen for 12 h. The white precipitate was filtered off. The pale yellow solution was then evaporated to dryness under vacuum. The solid was washed with MeOH and diethyl ether. The product was dried in vacuo and collected as a white solid. Yield: 123 mg (34%). Positive-ion ESI-MS ion clusters at m/z 781 $\{M + H^+\}^+$.

BpyC2C6B2. The procedure was similar to that for the preparation of bpyC2B2, except that 6-biotinamidohexanoic acid *N*-hydroxysuccinimidyl ester[37] (835 mg, 1.84 mmol) was used instead of biotinyl-*N*-hydroxysuccinimidyl ester. The product was collected as a white solid. Yield: 84 mg (18%). Positive-ion ESI-MS ion clusters at m/z 1007 $\{M + H^+\}^+$.

BpyC4. A mixture of bpy(COOMe)$_2$ (200 mg, 0.73 mmol) and *n*-butylamine (3.7 mL, 37 mmol) in CH_2Cl_2 (20 mL) was refluxed under an inert atmosphere of nitrogen for 12 h.

(35) Perrin, D. D.; Armarego, W. L. F. *Purification of Laboratory Chemicals*; Pergamon: Oxford, 1997.
(36) Peek, B. M.; Ross, G. T.; Edwards, S. W.; Meyer, G. J.; Meyer, T. J.; Erickson, B. W. *Int. J. Pept. Prot. Res.* **1991**, *38*, 114–123.
(37) Wilchek, M.; Bayer, E. A. *Methods Enzymol.* **1990**, *184*, 123–138.
(38) Sabatino, G.; Chinol, M.; Paganelli, G.; Papi, S.; Chelli, M.; Leone, G.; Papini, A. M.; De Luca, A.; Ginanneschi, M. *J. Med. Chem.* **2003**, *46*, 3170–3173.
(39) Ohsawa, Y.; Sprouse, S.; King, K. A.; DeArmond, M. K.; Hanck, K. W.; Watts, R. J. *J. Phys. Chem.* **1987**, *91*, 1047–1054.

The mixture was evaporated to dryness to give a pale yellow solid. The solid was then dissolved in chloroform, and the solution was washed with water, dried over anhydrous $MgSO_4$, and evaporated to dryness. Subsequent recrystallization from CH_2Cl_2/diethyl ether afforded the product as white crystals. Yield: 166 mg (64%). Positive-ion ESI-MS ion clusters at m/z 355 $\{M + H^+\}^+$.

[Ir(pba)$_2$(bpyC6B)](PF$_6$). A mixture of $[Ir_2(pba)_4Cl_2]$[24c] (71 mg, 0.06 mmol) and bpyC6B[24h] (65 mg, 0.12 mmol) in CH_2Cl_2/MeOH (80 mL, 1:3, v/v) was refluxed under an inert atmosphere of nitrogen in the dark for 12 h. The orange-red solution was then cooled to room temperature, and KPF_6 (24 mg, 0.13 mmol) was added to the solution. The mixture was stirred for 10 min at room temperature and then evaporated to dryness. The orange-red solid was dissolved in CH_3CN and purified by column chromatography on alumina. The desired product was eluted with CH_3CN/MeOH (4:1, v/v). Subsequent recrystallization from CH_2Cl_2/diethyl ether afforded [Ir(pba)$_2$(bpyC6B)](PF$_6$) as orange crystals. Yield: 108 mg (73%). ^{1}H NMR (300 MHz, DMSO-d_6, 298 K, TMS): δ 9.70 (s, 2H, CHO), 9.07 (s, 1H, H3 of bpy), 8.95 (t, 1H, J = 5.4 Hz, bpy-4-CON*H*), 8.83 (s, 1H, H3′ of bpy), 8.46 (d, 2H, J = 8.5 Hz, H5 of phenyl ring of pba), 8.18 (d, 2H, J = 7.9 Hz, H3 of pyridyl ring of pba), 8.06 (t, 2H, J = 7.8 Hz, H4 of pyridyl ring of pba), 7.93−7.86 (m, 2H, H5 and H6 of bpy), 7.80−7.71 (m, 2H, H5′ and H6′ of bpy), 7.68 (d, 2H, J = 5.6 Hz, H6 of pyridyl ring of pba), 7.59−7.51 (m, 3H, H6 of phenyl ring of pba and N*H*-biotin), 7.30 (q, 2H, J = 5.6 Hz, H5 of pyridyl ring of pba), 6.63 (d, 2H, J = 6.2 Hz, H2 of phenyl ring of pba), 6.42 (s, 1H, NH of biotin), 6.35 (s, 1H, NH of biotin), 4.36−4.27 (m, 1H, NCH of biotin), 4.19−4.10 (m, 1H, NCH of biotin), 3.06−2.98 (m, 3H, SCH of biotin and C*H*$_2$NH-biotin), 2.76 (d, 1H, J = 4.7 Hz, SCH of biotin), 2.62 (s, 1H, SCH of biotin), 2.37−2.33 (m, 2H, NHC*H*$_2$C$_4$H$_8$CH$_2$NHCO), 2.04 (t, 2H, J = 7.3 Hz, COC*H*$_2$C$_3$H$_6$ biotin), 1.56−1.21 (m, 14H, NHCH$_2$C$_4$*H*$_8$CH$_2$NHCO and COCH$_2$C$_3$*H*$_6$ of biotin). IR (KBr) ν/cm^{-1}: 3431 (br s, N−H), 1685 (s, C=O), 845 (s, PF_6^-). Positive-ion ESI-MS ion clusters at m/z 1095 $\{M^+\}^+$.

[Ir(ppyC6B)$_2$(bpy)](PF$_6$) (1). A mixture of [Ir(pba)$_2$(bpy)](PF$_6$)[24c] (86 mg, 0.10 mmol), *N*-biotinyl-1,6-diaminohexane[38] (137 mg, 0.40 mmol), and triethylamine (200 μL) in MeOH (50 mL) was refluxed under an inert atmosphere of nitrogen in the dark for 2 h. After the yellow solution was cooled to room temperature, a solid sample of $NaBH_4$ (61 mg, 1.6 mmol) was added to the solution. The solution was then stirred under an inert atmosphere of nitrogen for 12 h and then evaporated to dryness. The remaining solid was dissolved in CH_2Cl_2 (50 mL), and the solution was washed with distilled water (30 mL × 3). The CH_2Cl_2 layer was then dried over anhydrous $MgSO_4$, filtered, and evaporated to dryness to give a yellow solid. Subsequent recrystallization from acetone/diethyl ether afforded complex **1** as yellow crystals. Yield: 78 mg (52%). ^{1}H NMR (300 MHz, DMSO-d_6, 298 K, TMS): δ 8.86 (d, 2H, J = 9.1 Hz, H3 and H3′ of bpy), 8.25−8.17 (m, 4H, H4, H6, H4′, and H6′ of bpy), 8.20−7.80 (m, 6H, H5 and H5′ of bpy, H3 and H4 of pyridyl ring of ppy), 7.73−7.67 (m, 4H, H6 of phenyl ring of ppy and N*H*-biotin), 7.56 (d, 2H, J = 5.3 Hz, H6 of pyridyl ring of ppy), 7.10 (t, 2H, J = 6.2 Hz, H5 of pyridyl ring of ppy), 6.95 (d, 2H, J = 8.2 Hz, H5 of phenyl ring of ppy), 6.42 (s, 2H, NH of biotin), 6.36 (s, 2H, NH of biotin), 6.15 (s, 2H, H3 of phenyl ring of ppy), 4.32−4.22 (m, 2H, NCH of biotin), 4.15−4.05 (m, 2H, NCH of biotin), 3.42 (s, 4H, ppy-4-C*H*$_2$NH), 3.14−2.97 (m, 6H, SCH of biotin and C*H*$_2$NH-biotin), 2.79−2.74 (m, 2H, SCH of biotin), 2.56 (s, 2H, SCH of biotin), 2.29−2.24 (m, 4H, NHC*H*$_2$C$_4$H$_8$CH$_2$NHCO), 2.00 (t, 4H, J = 7.0 Hz, COC*H*$_2$C$_3$H$_6$ of biotin), 1.47−1.16 (m, 28H, NHCH$_2$C$_4$*H*$_8$CH$_2$NHCO and COCH$_2$C$_3$*H*$_6$ of biotin). IR (KBr) ν/cm^{-1}: 3424 (br s, N−H), 3273 (br s, N−H), 1698 (s, C=O), 845 (s, PF_6^-). Positive-ion ESI-MS ion clusters at m/z 694 $\{M^+ + Na^+\}^{2+}$. Anal. Calcd for $IrC_{66}H_{84}N_{12}O_4S_2PF_6 \cdot H_2O$: C, 51.85; H, 5.67; N, 10.99. Found: C, 52.14; H, 5.43; N, 10.79.

[Ir(ppy)$_2$(bpyC2B2)](PF$_6$) (2). A mixture of $[Ir_2(ppy)_4Cl_2]$[39] (32 mg, 0.03 mmol) and bpyC2B2 (47 mg, 0.06 mmol) in MeOH/CH_2Cl_2 (40 mL, 3:1, v/v) was refluxed under an inert atmosphere of nitrogen in the dark for 4 h. The red solution was then cooled to room temperature, and KPF_6 (13 mg, 0.07 mmol) was added to the solution. The mixture was stirred for 10 min at room temperature and then evaporated to dryness. The red solid was dissolved in MeOH/CH_2Cl_2 and purified by column chromatography on alumina. The desired product was eluted with CH_3CN/MeOH (1:1, v/v). Subsequent recrystallization from MeOH/diethyl ether afforded complex **2** as red crystals. Yield: 48 mg (56%). ^{1}H NMR (300 MHz, methanol-d_4, 298 K, TMS): δ 9.15 (s, 2H, H3 and H3′ of bpy), 8.16−8.14 (m, 4H, H6 and H6′ of bpy and H3 of pyridyl ring of ppy), 7.91−7.85 (m, 6H, H5 and H5′ of bpy and H6 of pyridyl ring and H6 of phenyl ring of ppy), 7.65 (t, 2H, J = 5.3 Hz, H4 of pyridyl ring of ppy), 7.10−7.04 (m, 4H, H5 of pyridyl ring and H5 of phenyl ring of ppy), 6.92 (t, 2H, J = 7.2 Hz, H4 of phenyl ring of ppy), 6.29 (d, 2H, J = 7.9 Hz, H3 of phenyl ring of ppy), 4.49−4.45 (m, 2H, NCH of biotin), 4.30−4.26 (m, 2H, NCH of biotin), 3.53−3.37 (m, 8H, NH(C*H*$_2$)$_2$NH), 3.13−3.07 (m, 2H, SCH of biotin), 2.89−2.83 (m, 2H, SCH of biotin), 2.65−2.61 (m, 2H, SCH of biotin), 2.23−2.17 (m, 4H, COC*H*$_2$ of biotin), 1.60−1.31 (m, 12H, COCH$_2$C$_3$*H*$_6$ of biotin). IR (KBr) ν/cm^{-1}: 3283 (br s, N−H), 1690 (s, C=O), 846 (s, PF_6^-). Positive-ion ESI-MS ion clusters at m/z 1280 $\{M^+\}^+$. Anal. Calcd for $IrC_{58}H_{62}N_{12}O_6S_2PF_6 \cdot 3H_2O$: C, 47.12; H, 4.64; N, 11.37. Found: C, 46.93; H, 4.92; N, 11.32.

[Ir(ppy)$_2$(bpyC2C6B2)](PF$_6$) (3). The procedure was similar to that for the preparation of complex **2**, except that bpyC2C6B2 (60 mg, 0.06 mmol) was used instead of bpyC2B2. Subsequent recrystallization from MeOH/diethyl ether afforded complex **3** as red crystals. Yield: 74 mg (75%). ^{1}H NMR (300 MHz, methanol-d_4, 298 K, TMS): δ 9.13 (s, 2H, H3 and H3′ of bpy), 8.16−8.14 (m, 4H, H6 and H6′ of bpy and H3 of pyridyl ring of ppy), 7.90−7.84 (m, 6H, H4 and H6 of pyridyl ring and H6 of phenyl ring of ppy), 7.65 (d, 2H, J = 5.3 Hz, H5, H5′ of bpy), 7.09−7.04 (m, 4H, H5 of pyridyl ring and H5 of phenyl ring of ppy), 6.92 (t, 2H, J = 7.5 Hz, H4 of phenyl ring of ppy), 6.29 (d, 2H, J = 7.9 Hz, H3 of phenyl ring of ppy), 4.50−4.42 (m, 2H, NCH of biotin), 4.31−4.23 (m, 2H, NCH of biotin), 3.50−3.44 (m, 8H, NH(C*H*$_2$)$_2$NH), 3.21−3.06 (m, 6H, SCH of biotin and C*H*$_2$NH-biotin), 2.92−2.87 (m, 2H, SCH of biotin), 2.69−2.65 (m, 2H, SCH of biotin), 2.21−2.13 (m, 8H, COC*H*$_2$), 1.67−1.28 (m, 24H, CONHCH$_2$C$_3$*H*$_6$CH$_2$NHCOCH$_2$C$_3$*H*$_6$). IR (KBr) ν/cm^{-1}: 3283 (br s, N−H), 1650 (s, C=O), 845 (s, PF_6^-). Positive-ion ESI-MS ion clusters at m/z 1506 $\{M^+\}^+$. Anal. Calcd for $IrC_{70}H_{86}N_{14}O_8S_2PF_6 \cdot 3H_2O$: C, 49.26; H, 5.43; N, 11.49. Found: C, 49.09; H, 5.39; N, 11.40.

[Ir(ppyC6B)$_2$(bpyC6B)](PF$_6$) (4). The procedure was similar to that for the preparation of complex **1**, except that [Ir(pba)$_2$(bpyC6B)](PF$_6$) (99 mg, 0.08 mmol) was used instead of [Ir(pba)$_2$(bpy)](PF$_6$). Subsequent recrystallization from MeOH/diethyl ether afforded complex **4** as orange crystals. Yield: 68 mg (45%). ^{1}H NMR (300 MHz, methanol-d_4, 298 K, TMS): δ 9.11 (s, 1H, H3 of bpy), 8.71 (s, 1H, H3′ of bpy), 8.14−8.12 (m, 3H, H6 of bpy and H3 of pyridyl ring of ppy), 7.87−7.81 (m, 6H, H5 and H6′ of bpy and H4 of pyridyl ring and H6 phenyl ring of ppy), 7.63 (t, 2H, J = 5.2 Hz, H6 of pyridyl ring of ppy), 7.43 (d, 1H, J = 5.6 Hz, H5′ of bpy), 7.14−6.98 (m, 4H, H5 of pyridyl ring and H5 of phenyl ring of ppy), 6.24 (d, 2H, J = 9.1 Hz, H3 of phenyl ring of ppy), 4.48−4.45 (m, 3H, NCH of biotin), 4.29−4.27 (m, 3H, NCH of biotin), 3.52−3.40 (m, 4H, ppy-4-C*H*$_2$NH), 3.15−3.13 (m, 9H, SCH of biotin and C*H*$_2$NH-biotin), 2.93−2.87 (m, 3H, SCH of biotin), 2.70−2.57 (m, 6H, CH_3 on C4′ bpy and SCH of biotin), 2.39−2.32 (m, 6H, NHC*H*$_2$C$_4$H$_8$CH$_2$NHCO), 2.19 (t, 6H, J = 7.2 Hz, COC*H*$_2$C$_3$H$_6$ of

biotin), 1.73−1.15 (m, 42H, $NHCH_2C_4H_8CH_2NHCO$ and $COCH_2C_3H_6$ of biotin). IR (KBr) ν/cm^{-1}: 3428 (br s, N−H), 3273 (br s, N−H), 1695 (s, C═O), 847 (s, PF_6^-). Positive-ion ESI-MS ion clusters at m/z 874 $\{M^+ + H^+\}^{2+}$. Anal. Calcd for $IrC_{84}H_{114}N_{16}O_7S_3PF_6 \cdot 3H_2O$: C, 51.81; H, 6.21; N, 11.51. Found: C, 51.60; H, 6.13; N, 11.66.

[Ir(ppy)$_2$(bpyC4)](PF$_6$) (5). The procedure was similar to that for the preparation of complex **2**, except that bpyC4 (21 mg, 0.06 mmol) was used instead of bpyC2B2. Subsequent recrystallization from CH_2Cl_2/diethyl ether afforded complex **5** as red crystals. Yield: 43 mg (72%). ^{1}H NMR (300 MHz, DMSO-d_6, 298 K, TMS): δ 9.19 (s, 2H, H3 and H3′ of bpy), 9.13 (t, 2H, J = 5.5 Hz, bpyCON*H*), 8.26 (d, 2H, J = 7.9 Hz, H3 of pyridyl ring of ppy), 7.99−7.90 (m, 8H, H6 and H6′ of bpy and H4 and H6 of pyridyl ring and H6 of phenyl ring of ppy), 7.65 (d, 2H, J = 5.7 Hz, H5 and H5′ of bpy), 7.11 (t, 2H, J = 5.9 Hz, H5 of pyridyl ring of ppy), 7.02 (t, 2H, J = 8.1 Hz, H5 of phenyl ring of ppy), 6.90 (t, 2H, J = 7.5 Hz, H4 of phenyl ring of ppy), 6.15 (d, 2H, J = 6.5 Hz, H3 of phenyl ring of ppy), 3.44−3.41 (m, 4H, NHC-$H_2CH_2CH_2CH_3$), 1.54−1.46 (m, 4H, $NHCH_2CH_2CH_2CH_3$), 1.38−1.28 (m, 4H, $NHCH_2CH_2CH_2CH_3$), 0.88 (t, 6H, J = 7.3 Hz, $NHCH_2CH_2CH_2CH_3$). IR (KBr) ν/cm^{-1}: 3457 (br s, N−H), 1665 (s, C═O), 840 (s, PF_6^-). Positive-ion ESI-MS ion clusters at m/z 854 $\{M^+\}^+$. Anal. Calcd for $IrC_{42}H_{42}N_6O_2PF_6$: C, 50.45; H, 4.23; N, 8.40. Found: C, 50.37; H, 4.25; N, 8.66.

Physical Measurements and Instrumentation. ^{1}H NMR spectra were recorded on a Varian Mercury 300 MHz NMR spectrometer at 298 K. Positive-ion ESI mass spectra were recorded on a Perkin- Elmer Sciex API 365 mass spectrometer. IR spectra were recorded on a Perkin-Elmer 1600 series FT-IR spectrophotometer. Elemental analyses were carried out on a Vario EL III CHN elemental analyzer. Electronic absorption, steady-state emission spectra were recorded on a Hewlett-Packard 8453 diode array spectrophotometer and a SPEX FluoroLog 3-TCSPC spectrophotometer, respectively. Emission lifetimes were measured in the Fast MCS or TCSPC mode with a NanoLED N-340 or NanoLED N-375 as the excitation source, respectively. Unless specified, all the solutions for photophysical studies were degassed with no fewer than four successive freeze−pump−thaw cycles and stored in a 10 cm^3 round-bottomed flask equipped with a side arm 1 cm fluorescence cuvette and sealed from the atmosphere by a Rotaflo HP6/6 quick-release Teflon stopper. Luminescence quantum yields were measured by the optically dilute method[40] with an aerated aqueous solution of $[Ru(bpy)_3]Cl_2$ (Φ_{em} = 0.028, λ_{ex} = 455 nm)[41] as the standard solution. The electrochemical measurements were performed on a CH Instruments Electrochemical Workstation CHI750A. Cyclic voltammetry experiments were carried out at room temperature using a two-compartment glass cell with a working volume of 500 μL. A platinum gauze counter electrode was accommodated in the working electrode compartment. The working and reference electrodes were a glassy carbon electrode and a Ag/AgNO$_3$ (0.1 mol dm^{-3} ^{n}Bu$_4$NPF$_6$ in CH_3CN) electrode, respectively. The reference electrode compartment was connected to the working electrode compartment via a Luggin capillary. Solutions for electrochemical measurements were degassed with prepurified argon gas. All potentials were referred to SCE.

HABA Assays. To a mixture of HABA (300 μM) and avidin (7.6 μM) in 50 mM potassium phosphate buffer pH 7.4 (2 mL) were added 5 μL aliquots of the iridium(III) biotin complex (1.1 mM) in MeOH at 1 min intervals. The formation of the iridium-avidin adduct was indicated by a decrease in the absorbance at 500 nm because of the displacement of HABA molecules from the avidin by the complex. A plot of $-\Delta A_{500\ nm}$ versus [Ir]:[avidin] was constructed.

Emission Titrations. Avidin (10 μM) in 50 mM potassium phosphate buffer pH 7.4/MeOH (2 mL, 9:1, v/v) was titrated with the iridium(III) biotin complex (0.80 mM) in MeOH by additions of 5 μL aliquots at 1 min intervals. The solution was excited at 350 nm, and the emission intensity of the solution was measured.

Dissociation Assays. The dissociation of avidin-bound iridium(III) biotin complex was induced by addition of excess biotin (4 μmol) in 50 mM potassium phosphate buffer pH 7.4 (200 μL) to a mixture of the iridium(III) biotin complex (40 nmol) and avidin (20 and 25 nmol for complexes **1**−**3** and **4**, respectively) in 50 mM potassium phosphate buffer pH 7.4/MeOH (1.8 mL, 9:1, v/v). The kinetics of the dissociation was monitored by the decrease in emission intensity, and the reaction proceeded under pseudo-first-order conditions. The rate constants, k_{off}, were obtained by nonlinear least-squares fits of I_{obs} versus time t according to the following equation:[42]

$$I_{obs} = I_{min} + (I_{max} - I_{min}) \exp(-k_{off} t)$$

where I_{obs}, I_{max}, and I_{min} are the emission intensities of the apparent, initial, and final forms of the iridium(III) biotin complex, respectively.

Microsphere Assays for Avidin-Cross-Linking Properties. Carboxyl-functionalized microspheres (diameter: 10 μm, concentration: 1.05 g cm^{-3}) embedded with a green fluorescent dye (λ_{ex} = 480 nm; λ_{em} = 520 nm) were used to study the avidin-cross-linking properties of the biotin complexes. A 100 μL portion of the microsphere sample was centrifuged, and the solid was washed with 50 mM potassium phosphate buffer pH 7.4 (1 mL × 4). The microspheres were then resuspended in phosphate buffer (1 mL). Avidin (60 nmol) and EDC (0.3 nmol) in phosphate buffer (1 mL) were added to the microsphere suspension. The mixture was incubated at room temperature for 12 h. The conjugated microspheres were then collected by centrifugation, washed with phosphate buffer (1 mL × 6), and resuspended in the same buffer (200 μL) to give a microsphere stock solution. The biotin complex (0.9 nmol) in a mixture of anhydrous DMSO (5 μL) and phosphate buffer (155 μL) was added to the microsphere stock solution (40 μL). The mixture was incubated at room temperature for 12 h. A 20 μL portion of this mixture was pipetted onto a glass slide and examined by a laser-scanning confocal microscope (Carl Zeiss, LSM510) (λ_{ex} = 488 nm; λ_{em} = 505 nm).

HPLC Analysis for Avidin-Cross-Linking Properties. A 125 μL aliquot of the iridium(III) biotin complex (147 nmol) in a mixture of DMSO (7 μL) and phosphate buffer (118 μL) was added dropwise with a Hamilton syringe to a stirred solution of avidin (14.7 nmol) in phosphate buffer (50 μL). After the solution was incubated at room temperature for 30 min, it was analyzed by size-exclusion HPLC. The chromatographic system consisted of a Waters 600 pump (Waters Corp., Milford, MA, U.S.A.) equipped with a Rheodyne 7725i injector (Rohnert Park, CA, U.S.A.) with a 20 μL sample loop. The column was a Waters Protein Pak Glass 300SW size-exclusion column (8.0 × 300 mm, Waters Corp., Milford, MA, U.S.A.). The UV detector (Waters 996 photodiode array) was set at 280 nm. The mobile phase was composed of potassium phosphate (50 mM, pH 6.8), NaCl (300 mM), EDTA (1 mM), and NaN_3 (1 mM) in deionized water. The flow rate was 0.75 mL min^{-1}. Under these conditions, unmodified avidin was eluted at about 12.5 min.

Signal Amplification Studies. A 10 μL portion of nonfluorescent carboxyl-functionalized microspheres (diameter: 10 μm, concentration: 1.10 g cm^{-3}) were coated with avidin in the same way as described above in the preparation of green fluorescent microsphere-avidin conjugates. The avidin-coated

(40) Demas, J. N.; Crosby, G. A. *J. Phys. Chem.* **1971**, *75*, 991–1024.
(41) Nakamura, K. *Bull. Chem. Soc. Jpn.* **1982**, *55*, 2697–2705.
(42) Marek, M.; Kaiser, K.; Gruber, H. J. *Bioconjugate Chem.* **1997**, *8*, 560–566.

nonfluorescent microspheres were resuspended in phosphate buffer (1 mL) as a stock mixture. A 15 μL portion of the mixture was pipetted onto a glass slide and examined by a laser-scanning confocal microscope (Leica TCS SPE) (λ_{ex} = 488 nm; λ_{em} > 532 nm). The stock mixture was incubated with complex **3** (0.6 mmol) dissolved in a mixture of anhydrous DMSO (100 μL) and phosphate buffer (900 μL) for 15 min. The microspheres were then washed with DMSO/phosphate buffer (1 mL, 1:9, v/v) and phosphate buffer containing 0.1% BSA (1 mL) to remove excess complex and nonspecifically bound complex, respectively. The supernatant was removed after centrifugation. Then, the microspheres were incubated with an avidin solution in phosphate buffer (10 mg/1 mL) for 15 min and then washed with phosphate buffer (1 mL × 3) to remove excess avidin. Five cycles of alternative incubation with complex **3** and then with avidin were performed. After each cycle, the microspheres were resuspended in phosphate buffer (1 mL), and a 15 μL portion of the mixture was examined by confocal microscopy.

HPLC Analysis for Determination of Lipophilicity. The lipophilicity, which is referred to as log $P_{o/w}$ ($P_{o/w}$ = 1-octanol/water partition coefficient), of the complexes was determined from the log k'_w value (k'_w = chromatographic capacity factor at 100% aqueous solution). The log k'_w value was determined by reversed-phase HPLC on a C-18 column according to the method described by Minick.[43] The organic portion of the mobile phase was composed of MeOH and 0.25% 1-octanol. The aqueous portion was MOPS (0.02 M) buffer and 0.15% *n*-decylamine, adjusted to pH 7.4 with NaOH and then saturated with 1-octanol. The volumetric flow rate was 1 mL min^{-1}. The complex was dissolved in MeOH at a concentration of 100 μg/mL, and a volume of 20 μL was injected into the column. The k' value is defined as $(t_R - t_o)/t_o$, where t_R and t_o are the retention times of the complex and non-retained species (solvent), respectively. The log k'_w value was obtained from linear extrapolation of log k' versus ϕ MeOH (ϕ MeOH = the volume fraction of MeOH) data acquired in the region 0.50 ≤ ϕ MeOH ≤ 0.80. The log $P_{o/w}$ value of the complex was then determined from a standard curve (log $P_{o/w}$ vs log k'_w) constructed with data of standard compounds including 4-methoxyaniline, 4-methoxyphenol, phenol, acetophenone, naphthalene, *tert*-butylbenzene, anthracene, and pyrene with experimentally verified partition coefficients. The chromatographic system was the same as that used for avidin-cross-linking property analysis. The column was an Ultrasphere ODS column (250 mm × 4.6 mm, Beckman, Fullerton, CA, U.S.A.). The UV detector (Waters 996 photodiode array) was set at 280 nm.

MTT Assays. HeLa cells were seeded in a 96-well flat-bottomed microplate (10,000 cells/well) in growth medium (100 μL) and incubated at 37 °C under a 5% CO_2 atmosphere for 24 h. Detailed procedures for the cytotoxicity assays have been described previously.[24s] The absorbance of the solutions at 570 nm was measured with a SPECTRAmax 340 microplate reader (Molecular Devices Corp., Sunnyvale, CA). The IC_{50} value of the complex was determined from the dose dependence of surviving cells after exposure to the complex for 48 h.

ICP-MS. HeLa cells were grown in a 60 mm tissue culture dish and incubated at 37 °C under a 5% CO_2 atmosphere for 48 h. The culture medium was removed and replaced with medium/DMSO (99:1, v/v) containing the complex at a concentration of 5 μM. After incubation for 3 h, the medium was removed and the cell layer was washed gently with PBS (1 mL × 3). After that, the cell layer was trypsinized, digested in 65% HNO_3 (2 mL) at 70 °C for 2 h, and then diluted in Milli-Q water to the final volume of 10 mL for ICP-MS (PerkinElmer SCIEX, ELAN DRC Plus) analysis.

Live-Cell Confocal Imaging. HeLa cells were grown on sterile glass coverslips in a 60 mm tissue culture dish. The sample preparation procedure was similar to that of the ICP-MS. After washing with PBS, the coverslips were mounted onto slides for measurements. Imaging was performed using a confocal microscope (Leica TCS SPE) with an excitation wavelength at 405 nm. The emission was measured using a long-pass filter at 532 nm.

Flow Cytometry. The sample preparation procedure was similar to that of the ICP-MS. After washing with PBS, the cell layer was trypsinized and added up to a final volume of 3 mL with PBS. The samples were analyzed by a FACSCalibur flow cytometer (Becton, Dickinson and Co., Franklin Lakes, NJ, U.S.A.) with excitation at 488 nm. The number of cells analyzed for each sample was between 9,000 and 10,000.

Cell Fixation. HeLa cells were grown on sterile glass coverslips in a 60 mm tissue culture dish and incubated at 37 °C under a 5% CO_2 atmosphere for 48 h. The culture medium was removed and replaced with MeOH. After incubation for 15 min, the MeOH was removed and the cell layer was washed gently with PBS (5 mL × 3) and then incubated with PBS/DMSO (99:1, v/v) containing complex **5** (5 μM, 3 min). After washing with PBS, the coverslips were mounted onto slides for measurements. Imaging experiments were performed using a confocal microscope (Leica TCS SPE) with an excitation wavelength at 405 nm. The emission was measured using a long-pass filter at 532 nm.

Acknowledgment. We thank The Hong Kong Research Grants Council (Project No. CityU 101908) and City University of Hong Kong (Project No. 7002221) for financial support. K.Y.Z. acknowledges the receipt of a postgraduate studentship, a research tuition scholarship, and an outstanding academic performance award administered by the City University of Hong Kong. We thank Dr. Yun-Wah Lam for helpful discussion, Mr. Kenneth King-Kwan Lau, Mr. Michael Wai-Lun Chiang, and Mr. Ho-Hang Chan for their assistance on the cellular experiments, and Mr. Terence Kwok-Ming Lee for preliminary synthetic work of the ligands.

(43) Minick, D. J.; Frenz, J. H.; Patrick, M. A.; Brent, D. A. *J. Med. Chem.* **1988**, *31*, 1923–1933.